Probing dark matter substructure
using
gravitational microlensing

Djuna Lize Croon (IPPP Durham)

BNL remote seminar, June 2025

djuna.l.croon@durham.ac.uk | djunacroon.com

A key question for particle physics & cosmology

What on Earth is dark matter?

- Plenty of evidence!
- Likely not explained by modifications of gravity

https://youtu.be/IEKcPfJHfNU (see also djunacroon.com)

A key question for particle physics & cosmology

What on Earth is dark matter?

- Plenty of evidence!
- Likely not explained by modifications of gravity

https://youtu.be/IEKcPfJHfNU (see also djunacroon.com)

No idea, or too many ideas, about its nature:

Dark matter substructure

Two things we may agree upon…

- All of our evidence for dark matter is gravitational
- Many dark matter models feature substructure

PBHs | Boson stars | Subhalos | Miniclusters | Mirror stars

I call objects like these EDOs
(extended dark objects)

Dark matter substructure

Two things we may agree upon…

- All of our evidence for dark matter is gravitational
- Many dark matter models feature substructure

PBHs	Boson stars	Subhalos	Miniclusters	Mirror stars

- Microlensing can be used to probe such models

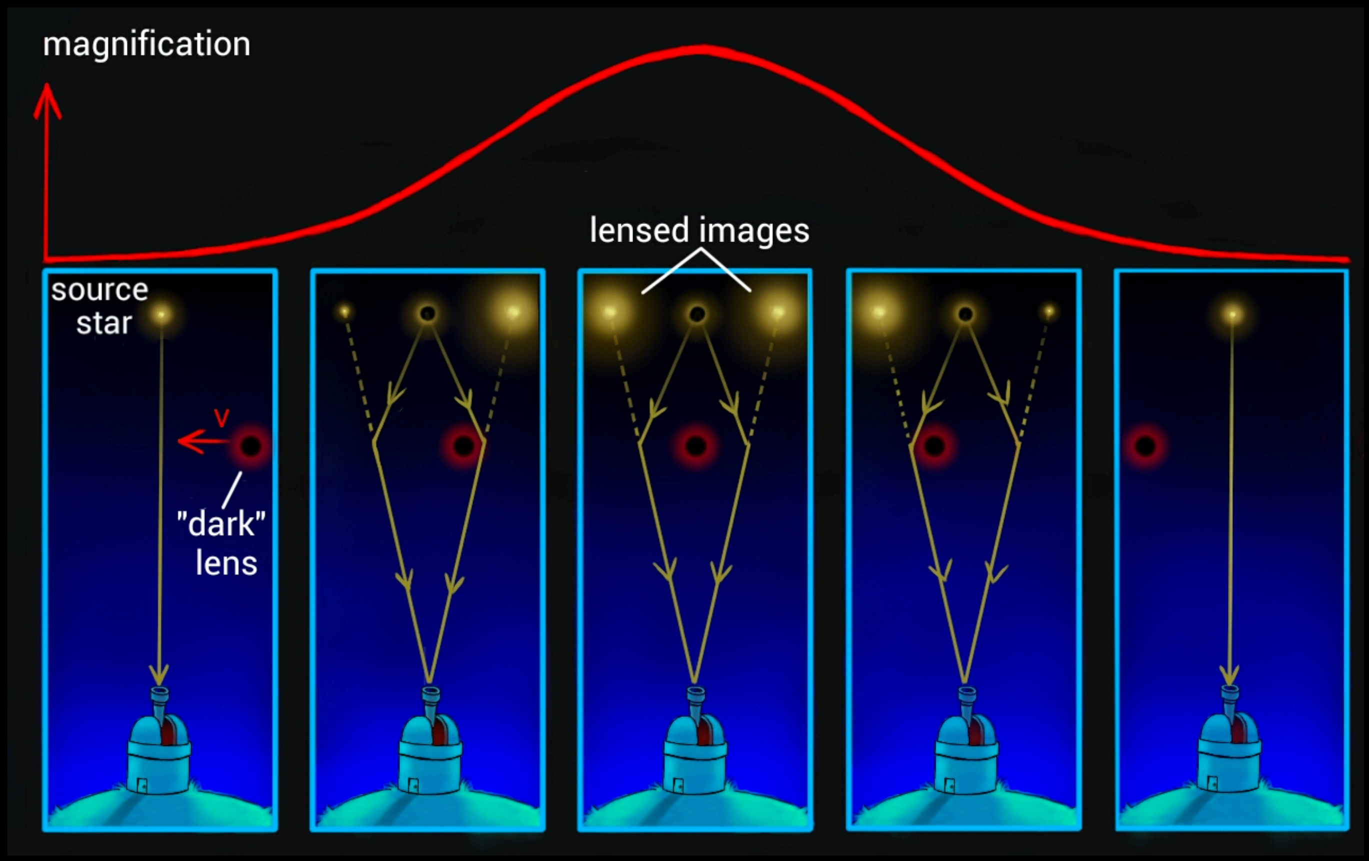

Image credit: Adam Rogers, theamateurrealist.wordpress.com

Geometry

"Thin screen approximation"

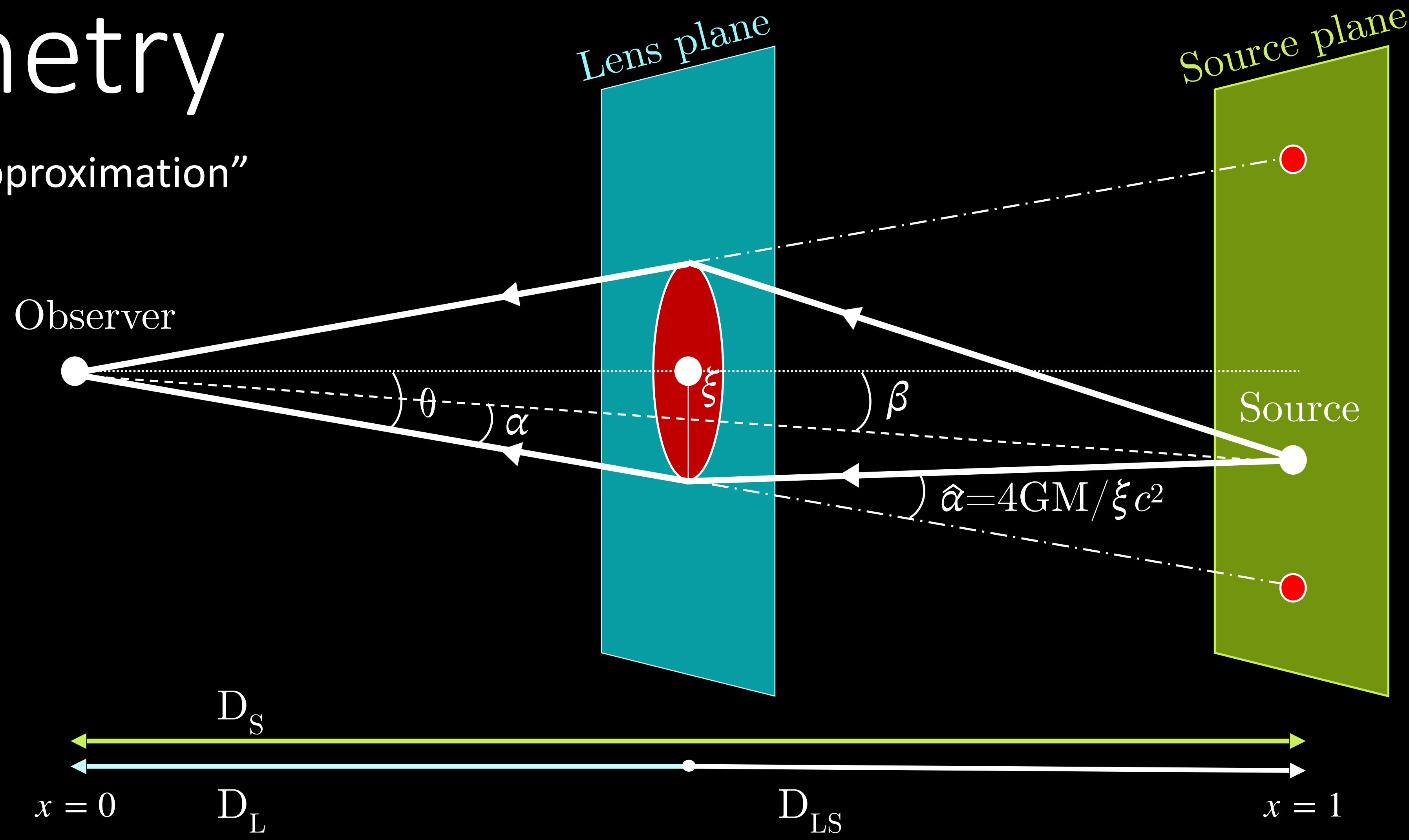

Geometry

"Thin screen approximation"

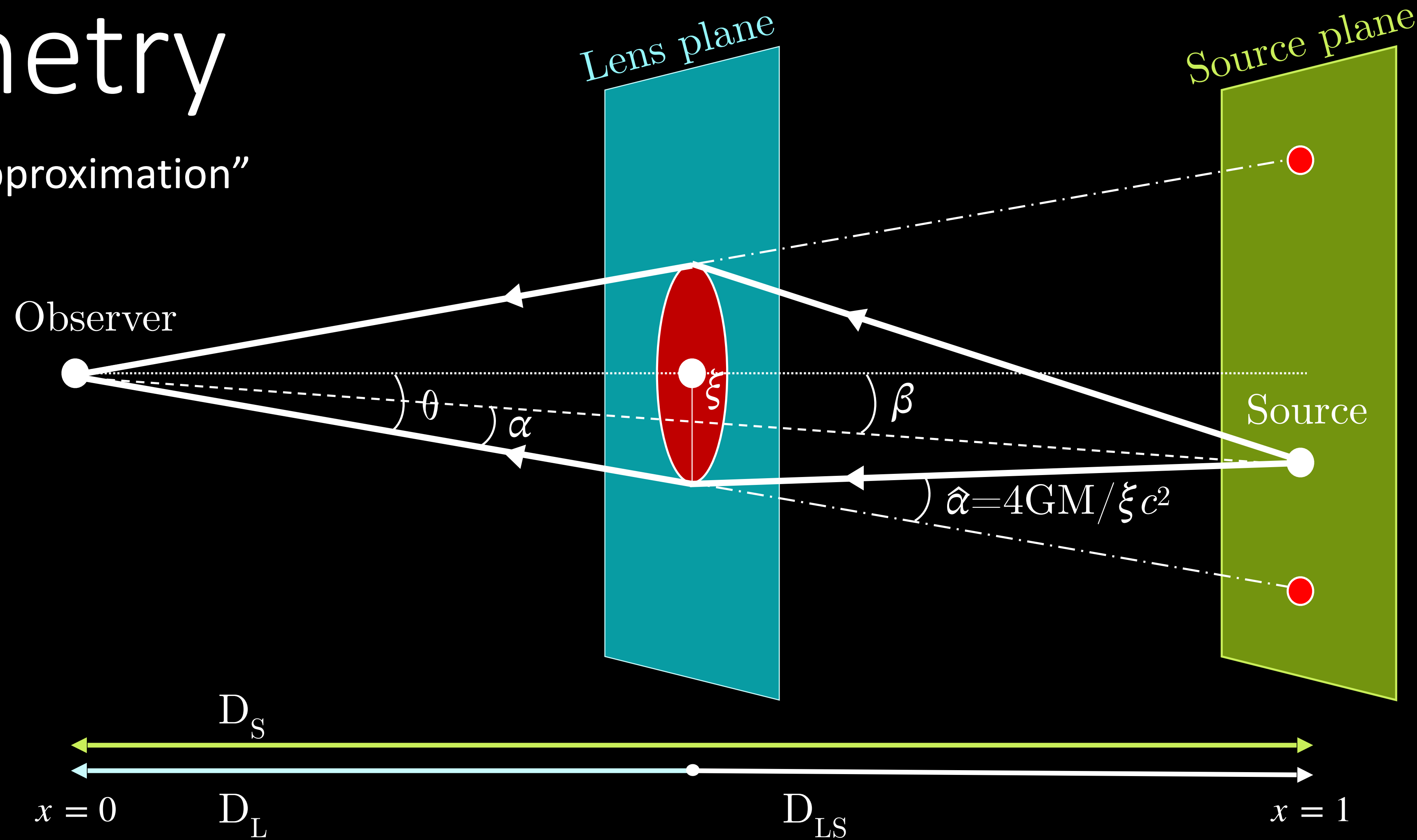

Lensing equation: $\beta = \theta - \frac{4GM(\theta)}{\theta D_L c^2} \frac{D_{LS}}{D_S}$

Magnification: $\mu = \frac{\theta}{\beta} \frac{d\theta}{d\beta} = \sum_i \mu_i$

Geometry

"Thin screen approximation"

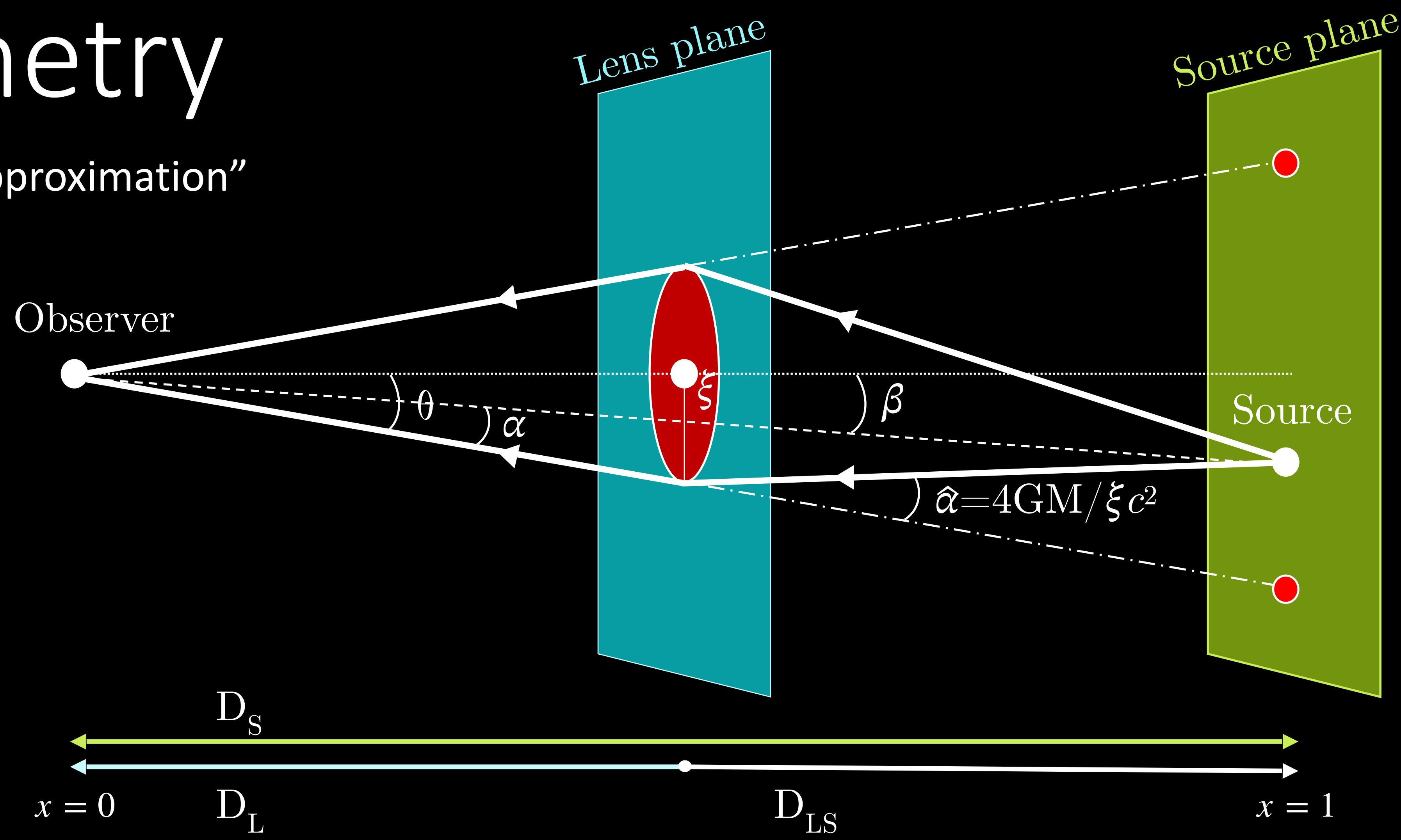

Lensing equation: $\beta = \theta - \frac{4GM(\theta)}{\theta D_L c^2}\frac{D_{LS}}{D_S}$

$$\beta = 0 \rightarrow \ \theta \equiv \theta_E = \sqrt{\frac{4GM}{c^2}\frac{D_{LS}}{D_L D_S}}$$

Magnification: $\mu = \frac{\theta}{\beta}\frac{d\theta}{d\beta} = \sum_i \mu_i$

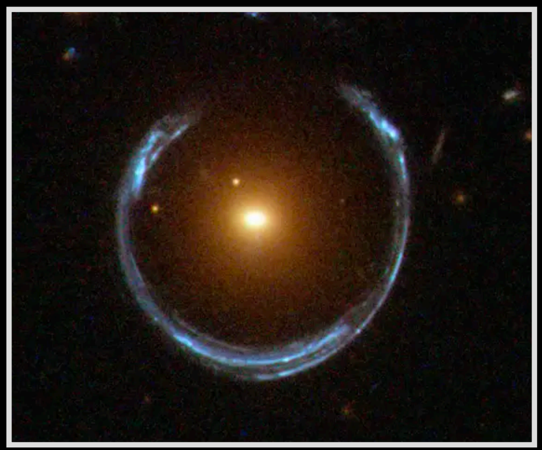

Einstein radius
$r_E = \theta_E D_L$

Near perfect Einstein Ring with the HST

Geometry

"Thin screen approximation"

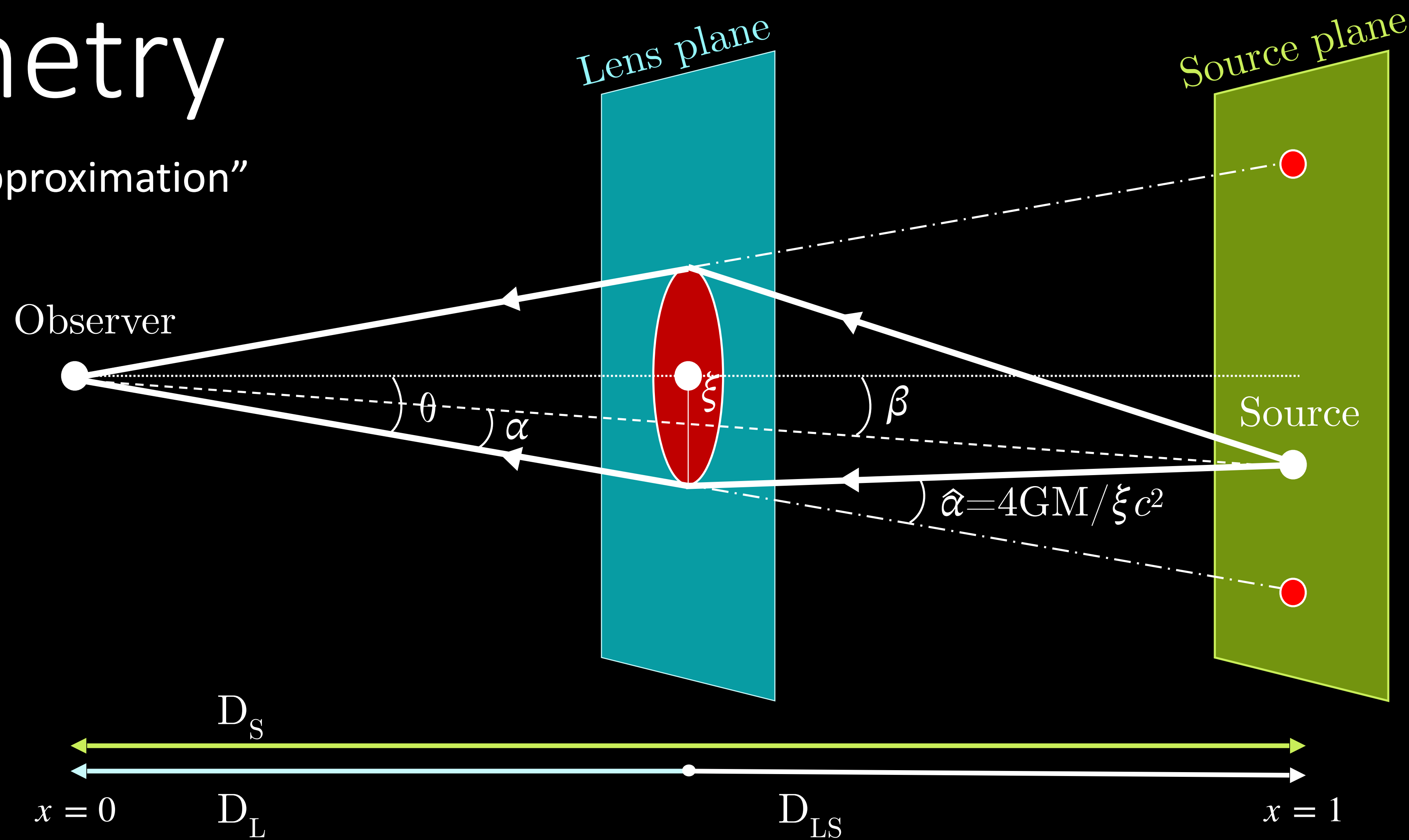

Normalise everything to θ_E

- $u \equiv \beta/\theta_E$
- $\tau \equiv \theta/\theta_E$
- $m(\tau) \equiv M(\theta_E \tau)/M$

Lensing equation: $u = \tau - \dfrac{m(\tau)}{\tau}$

Magnification: $\mu = \left|1 - \dfrac{m(\tau)}{\tau^2}\right|^{-1} \left|1 + \dfrac{m(\tau)}{\tau^2} - \dfrac{1}{\tau}\dfrac{dm(\tau)}{d\tau}\right|^{-1}$

Geometry

"Thin screen approximation"

$$m(\tau) = \frac{\int_0^\tau d\sigma\sigma \int_0^\infty d\lambda \rho(r_E\sqrt{\sigma^2+\lambda^2})}{\int_0^\infty d\gamma \gamma^2 \rho(r_E \gamma)}$$

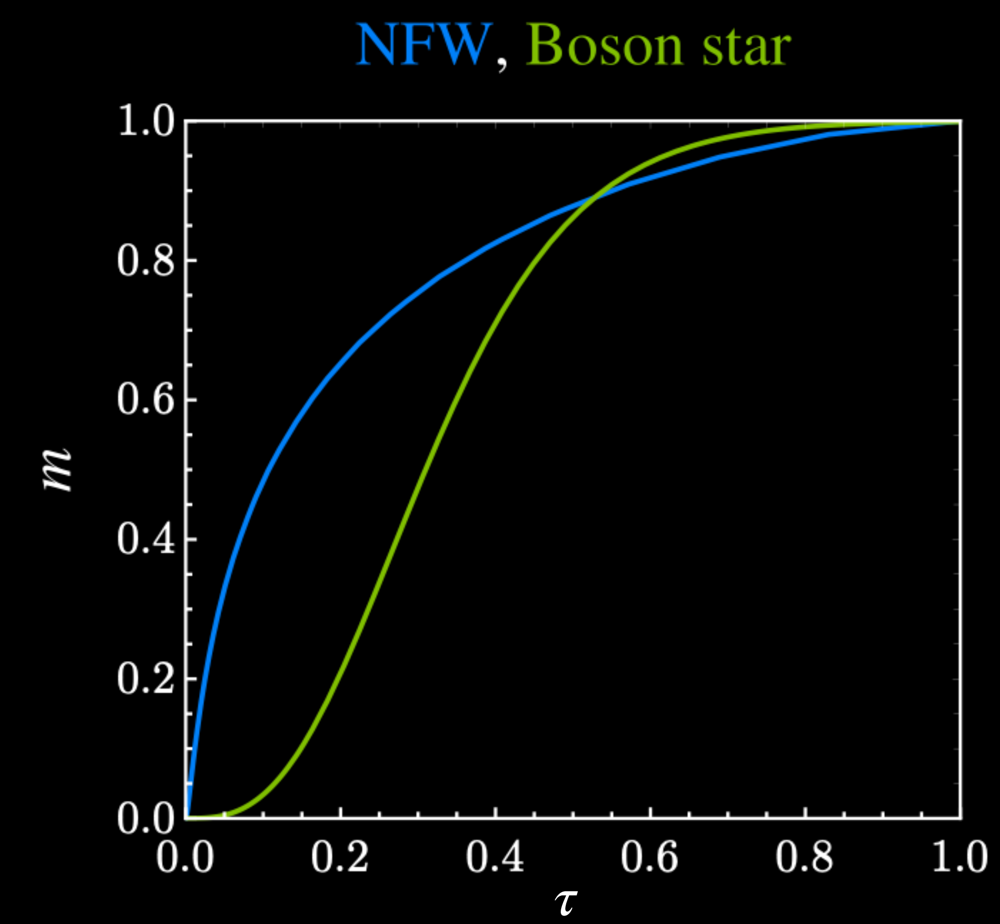

Projected lens mass distribution

Point-like lenses: $m(\tau) = 1$

Lensing equation: $u = \tau - \frac{m(\tau)}{\tau}$

Magnification: $\mu = \left|1 - \frac{m(\tau)}{\tau^2}\right|^{-1} \left|1 + \frac{m(\tau)}{\tau^2} - \frac{1}{\tau}\frac{dm(\tau)}{d\tau}\right|^{-1}$

Solving the lens equation $u = \tau - \frac{m(\tau)}{\tau}$

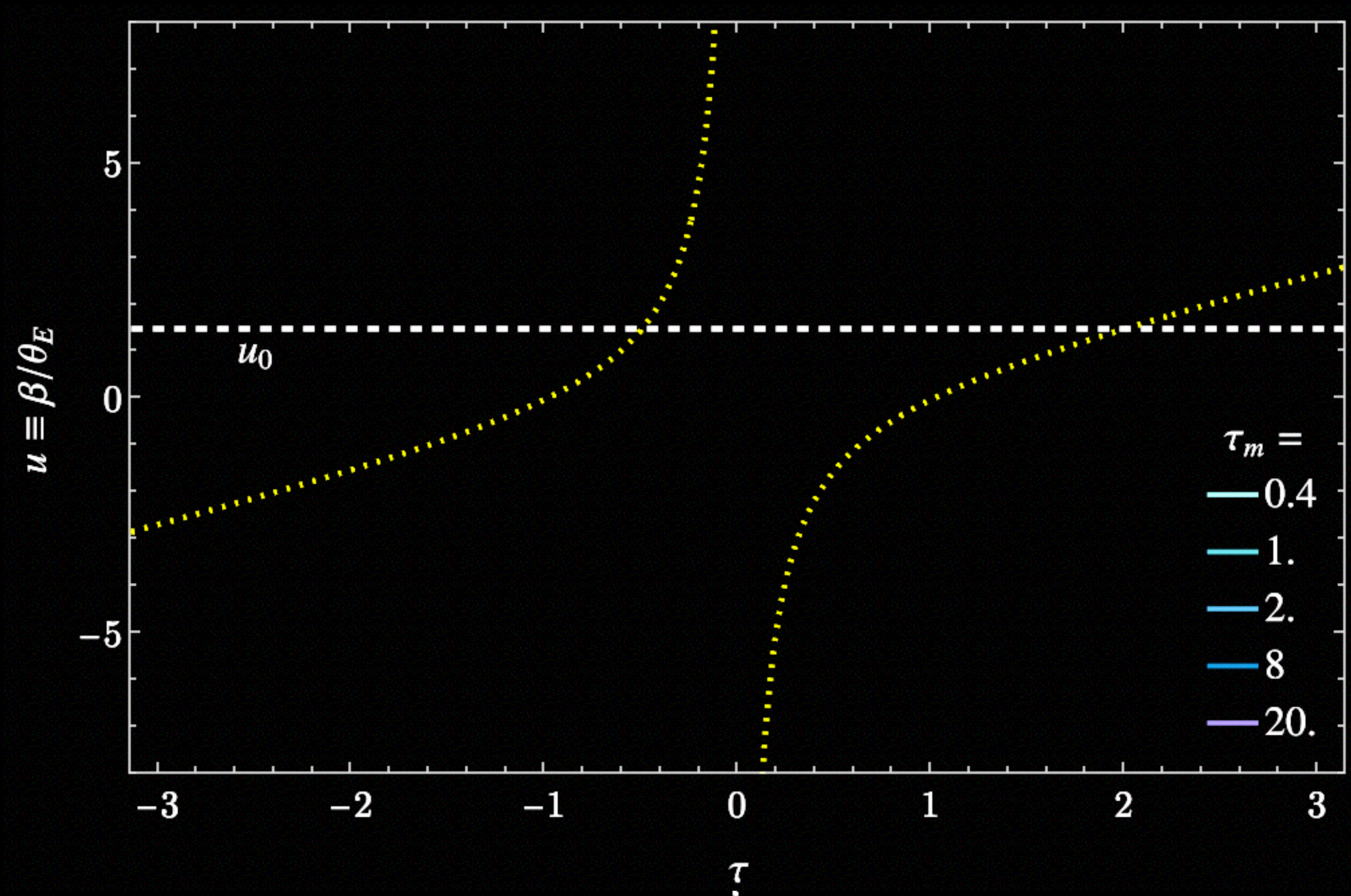

point-like

Solving the lens equation

$$u = \tau - \frac{m(\tau)}{\tau}$$

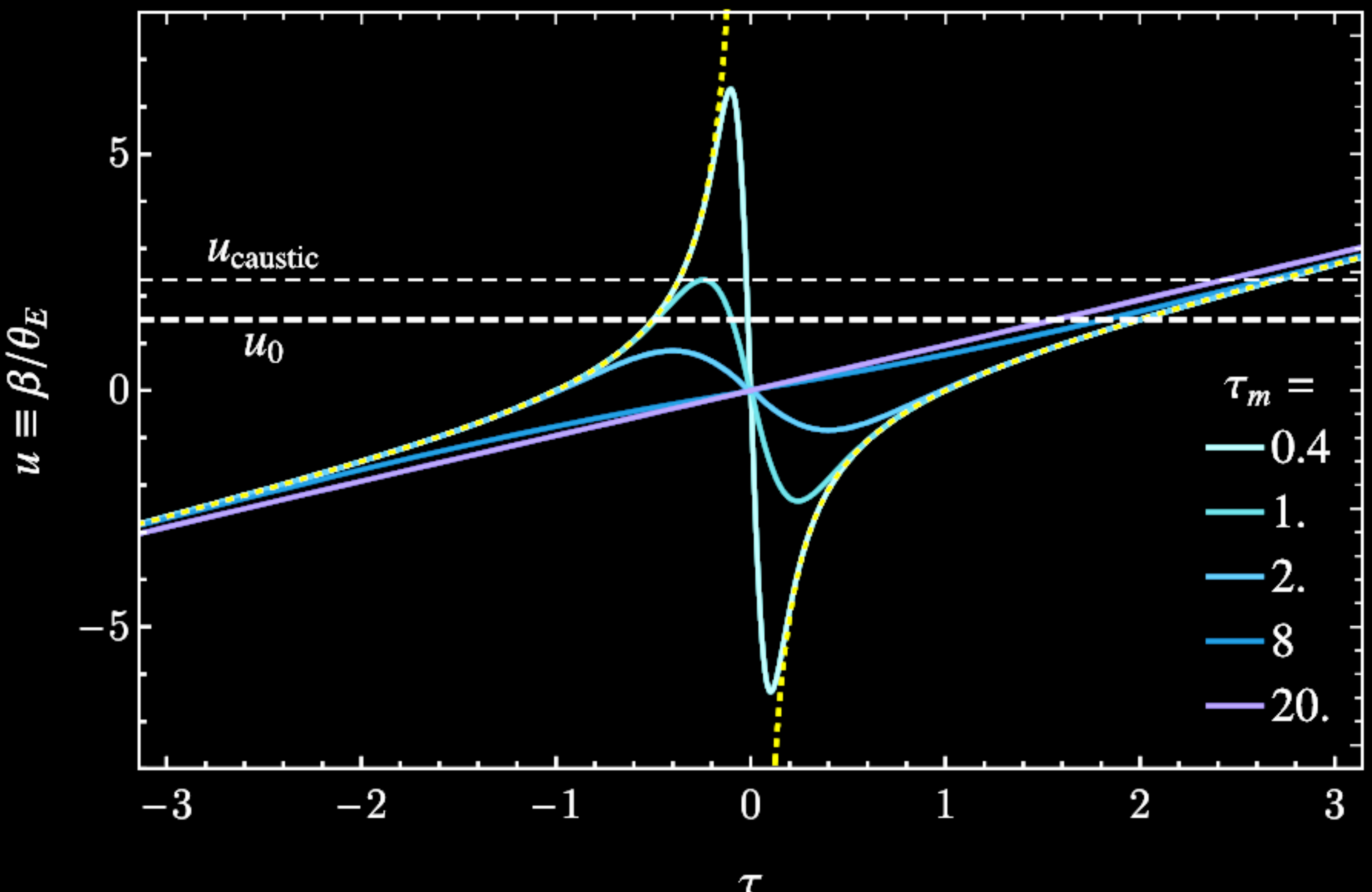

point-like

$$\tau_m \equiv \theta_{\rm lens}/\theta_E = r_{\rm lens}/r_E$$

Solving the lens equation $u = \tau - \frac{m(\tau)}{\tau}$

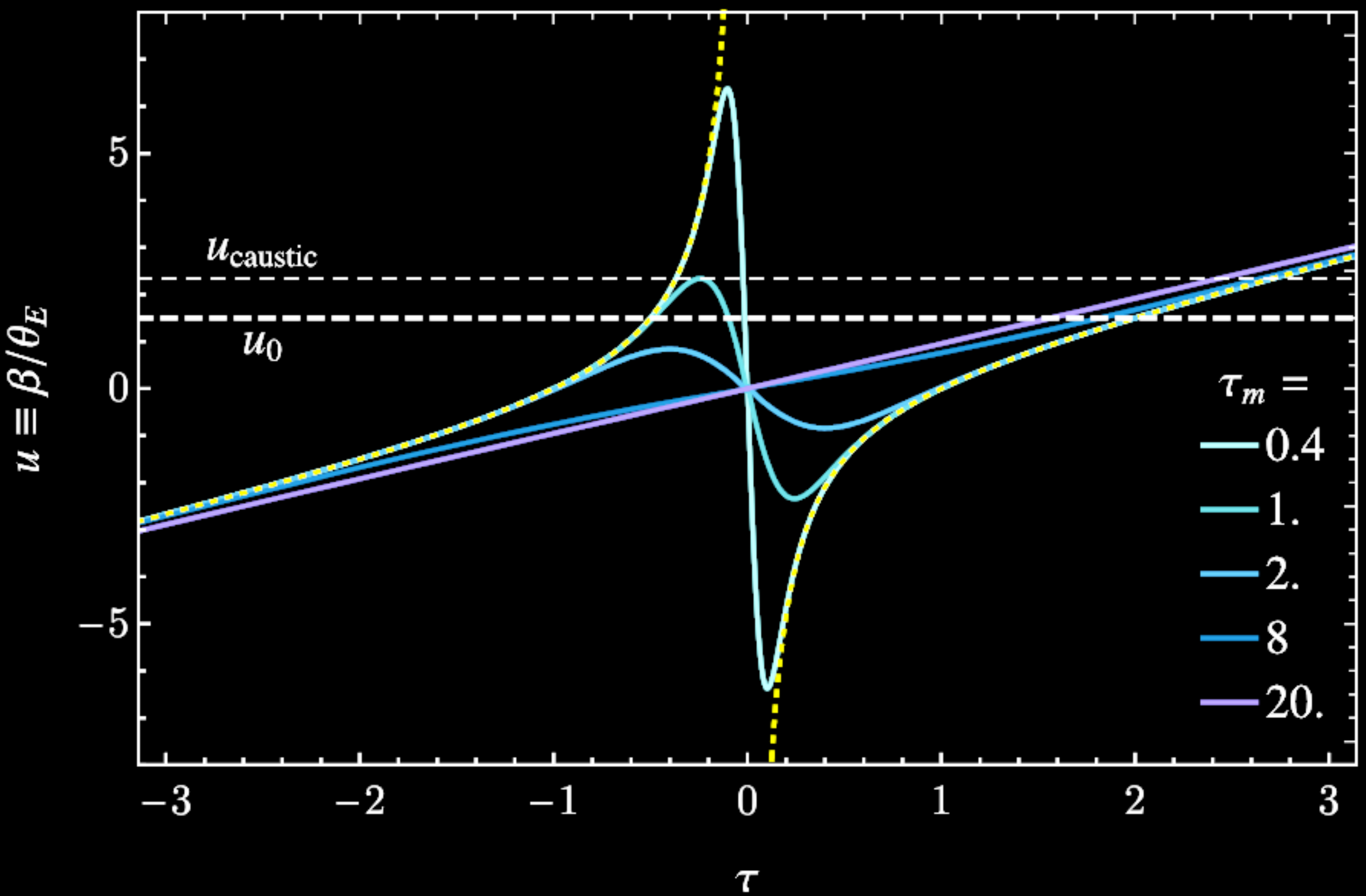

point-like

3 solutions, one with negligible μ_i

3 solutions, all contributing μ_i

1 solution of the point-like case

1 solution, larger μ_i than point-like

1 solution, $\mu_i \to 0$

→ at $u_{\rm caustic}$, number of solutions jumps from 1 to 3

Caustics

Example light curve

Boson star with $\tau_m = 1$

PBH (or $\tau_m = 0$)

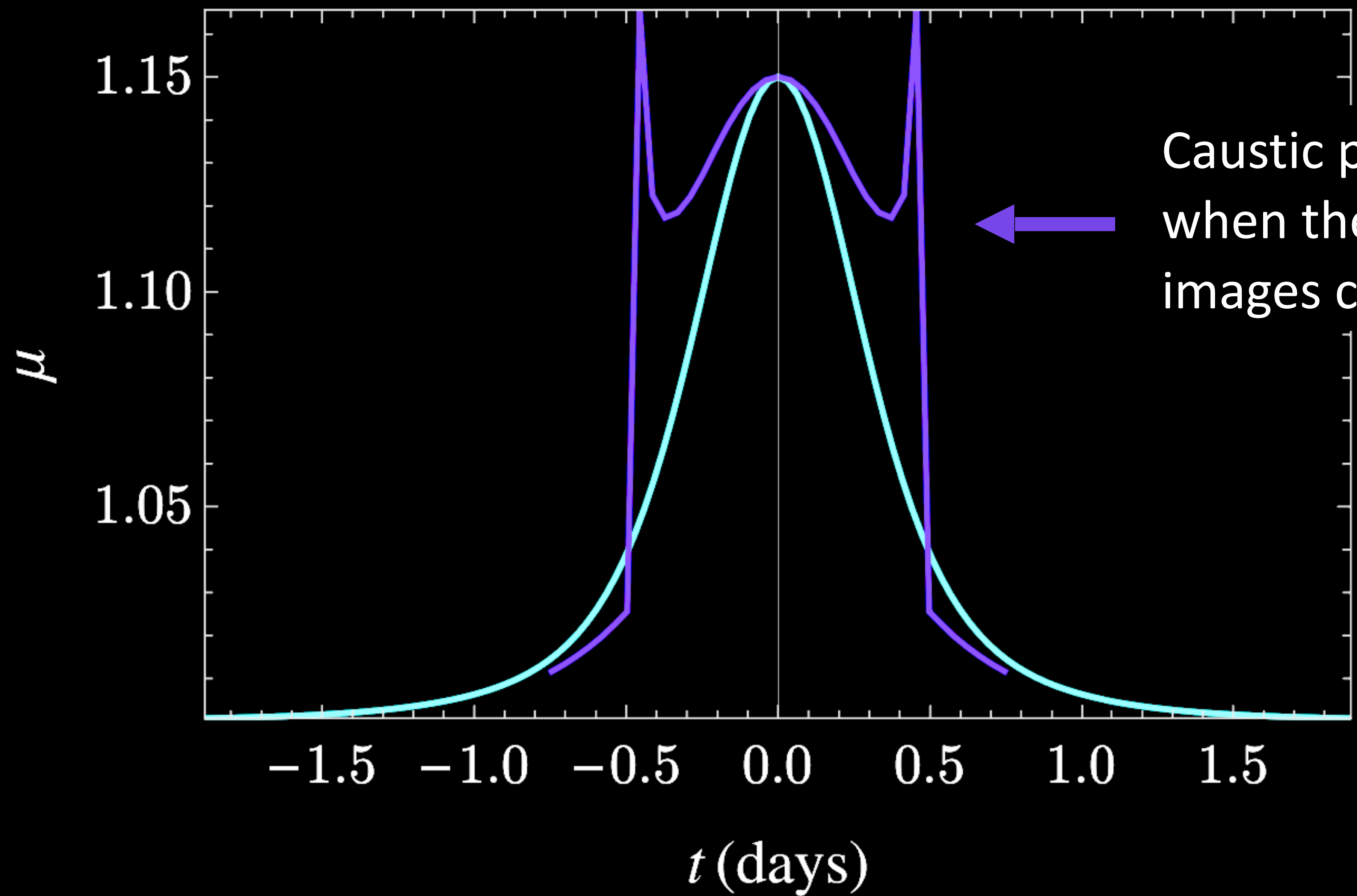

Caustic peaks arise when the number of images changes

Point-like lens: $m(\tau) = 1 \rightarrow \ \mu = \dfrac{u^2+2}{u\sqrt{u^2+4}}$

“Efficiency” of extended lenses

Define $u_{1.34}$ *by* $\mu_{\rm tot}(u \leq u_{1.34}) > 1.34$

The threshold impact parameter

All smaller impact parameters produce a magnification above $\mu > 1.34$

By definition $u_{1.34}$ is 1 for point-like lenses

DC, D. McKeen, N. Raj, PRD, arXiv:2002.08962 [astro-ph.CO]

"Efficiency" of extended lenses

Define $u_{1.34}$ *by* $\mu_{\text{tot}}(u \le u_{1.34}) > 1.34$

The threshold impact parameter

All smaller impact parameters produce a magnification above $\mu > 1.34$

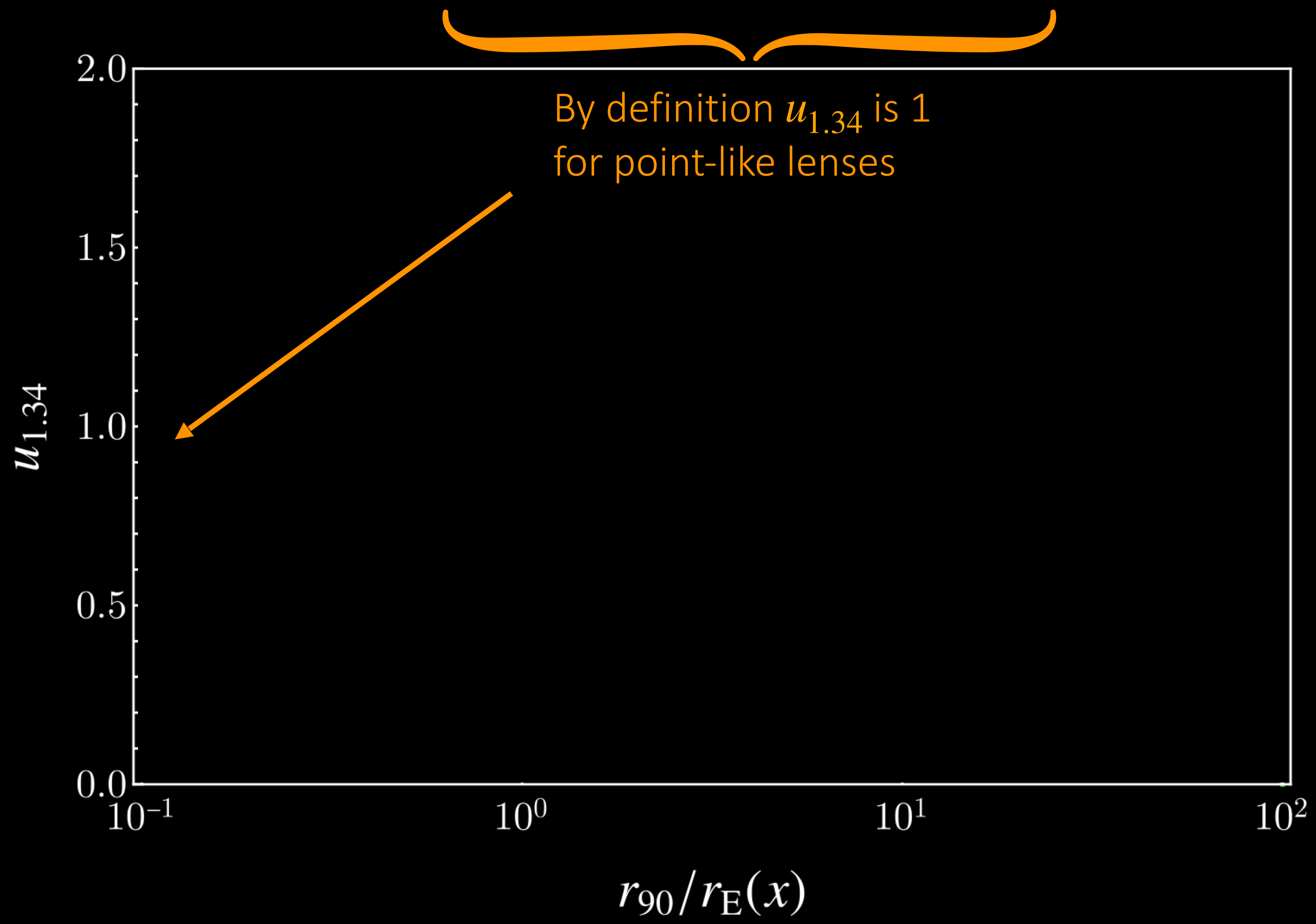

DC, D. McKeen, N. Raj, PRD, arXiv:2002.08962 [astro-ph.CO]

"Efficiency" of extended lenses

Define $u_{1.34}$ *by* $\mu_{\rm tot}(u \le u_{1.34}) > 1.34$

The threshold impact parameter

All smaller impact parameters produce a magnification above $\mu > 1.34$

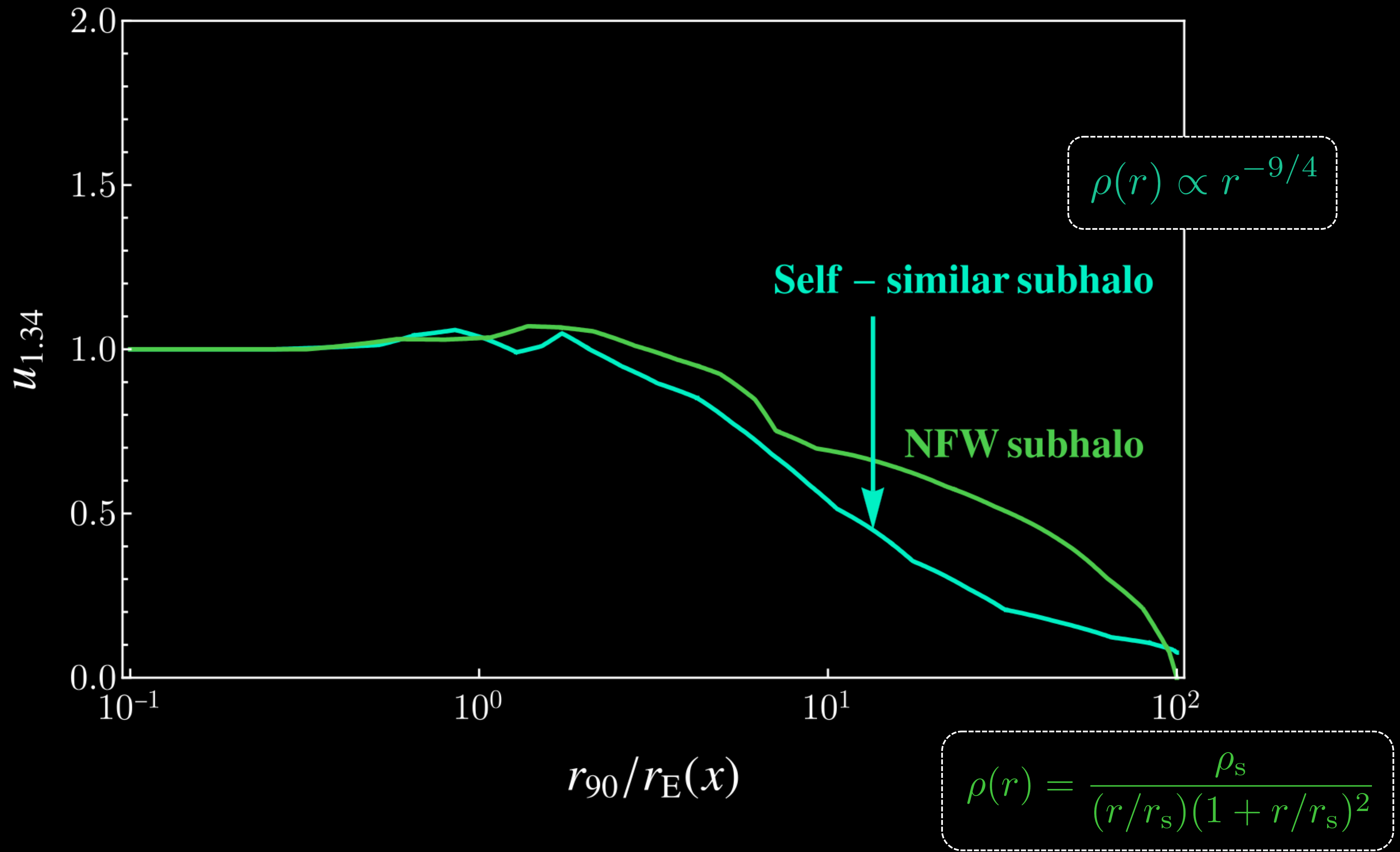

DC, D. McKeen, N. Raj, PRD, arXiv:2002.08962 [astro-ph.CO]

"Efficiency" of extended lenses

Define $u_{1.34}$ by $\mu_{\rm tot}(u \le u_{1.34}) > 1.34$

The threshold impact parameter

All smaller impact parameters produce a magnification above $\mu > 1.34$

Numerically solve the Schrodinger-Poisson equations

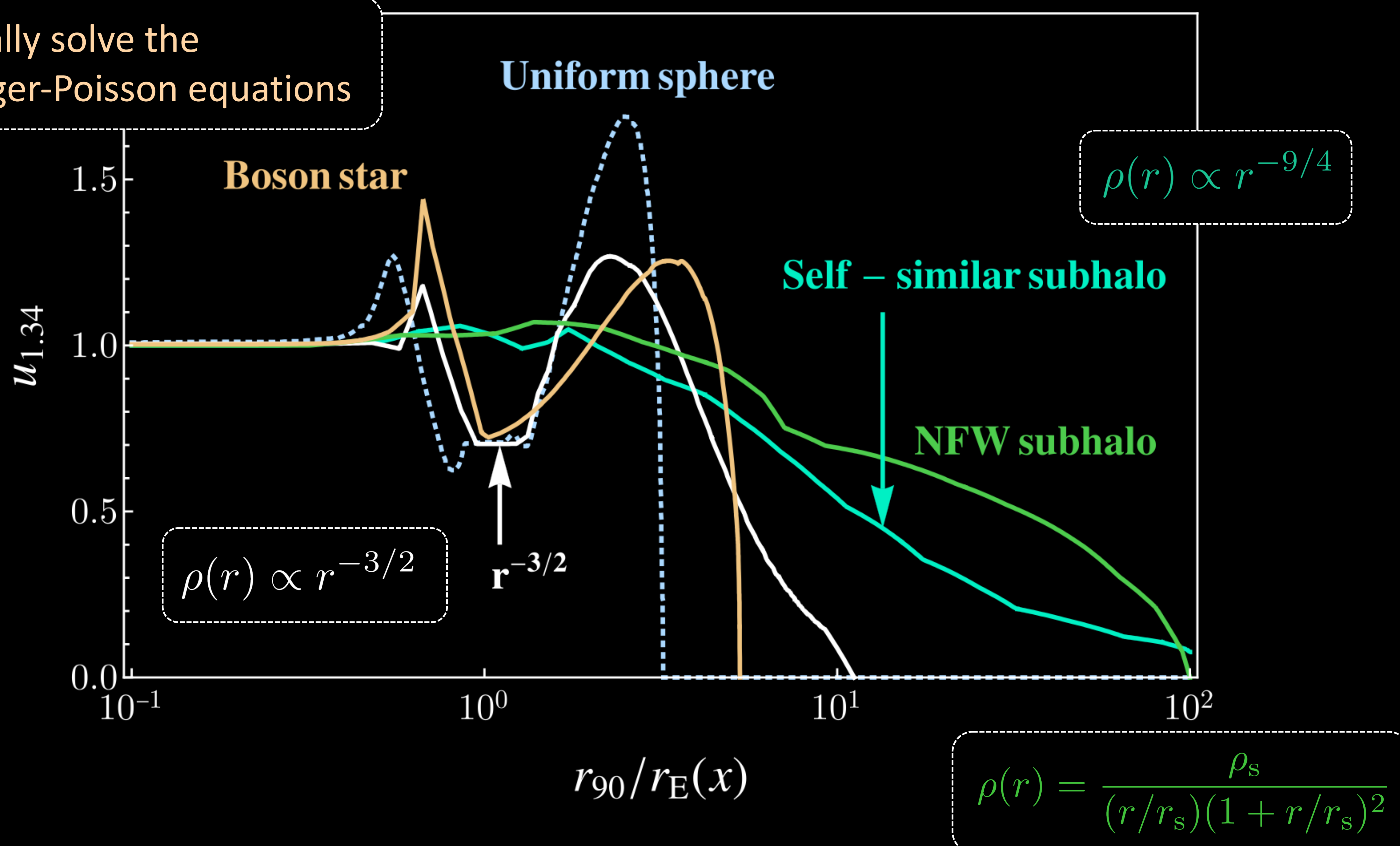

DC, D. McKeen, N. Raj, PRD, arXiv:2002.08962 [astro-ph.CO]

Constraints on DM fraction

Using the differential event rate, find constraints given expected number of (non-observed) events. Use derived efficiency for extended lenses.

As expected, constraints on extended objects are weaker…

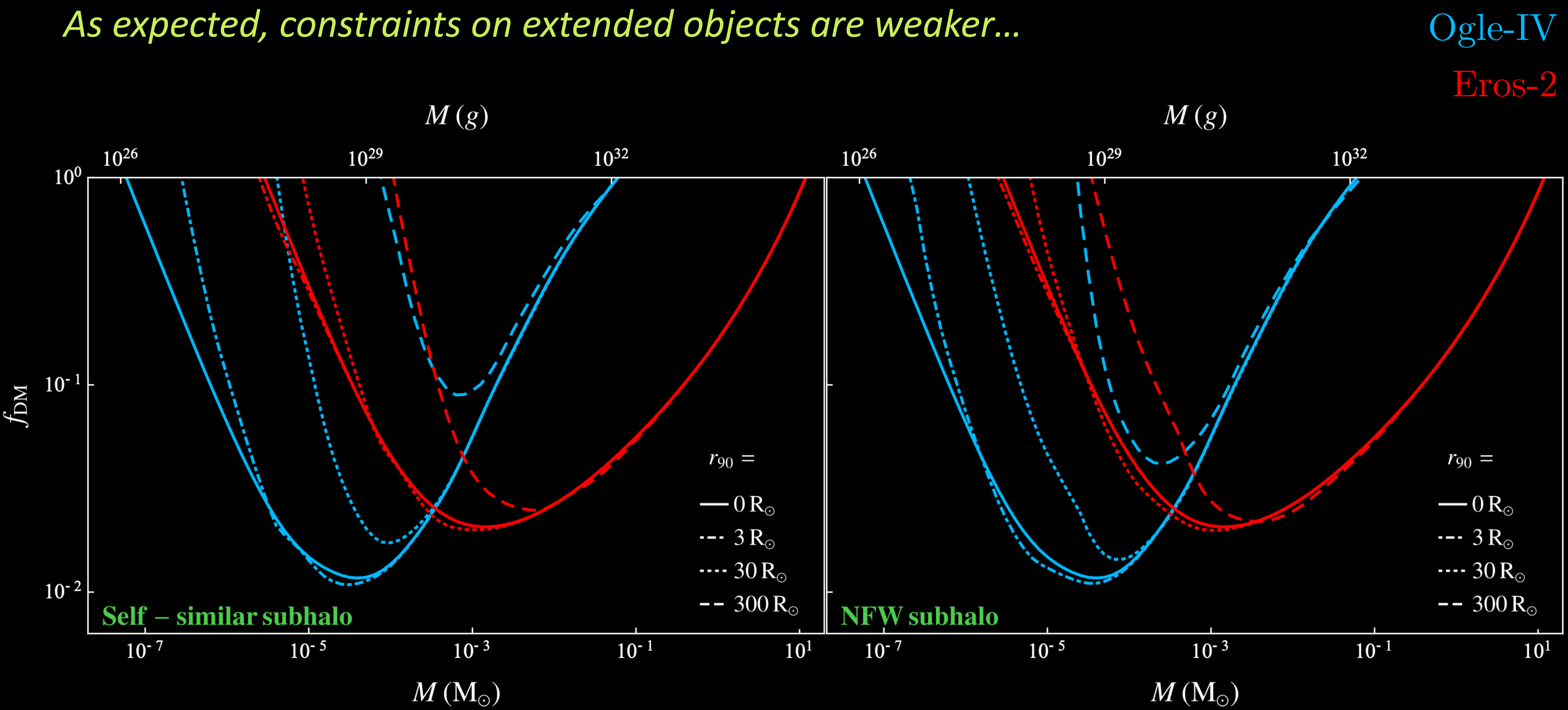

DC, D. McKeen, N. Raj, PRD, arXiv:2002.08962 [astro-ph.CO]

Constraints on DM fraction

Using the differential event rate, find constraints given expected number of (non-observed) events. Use derived efficiency for extended lenses.

But for sufficiently flat density profiles, caustics change the constraints

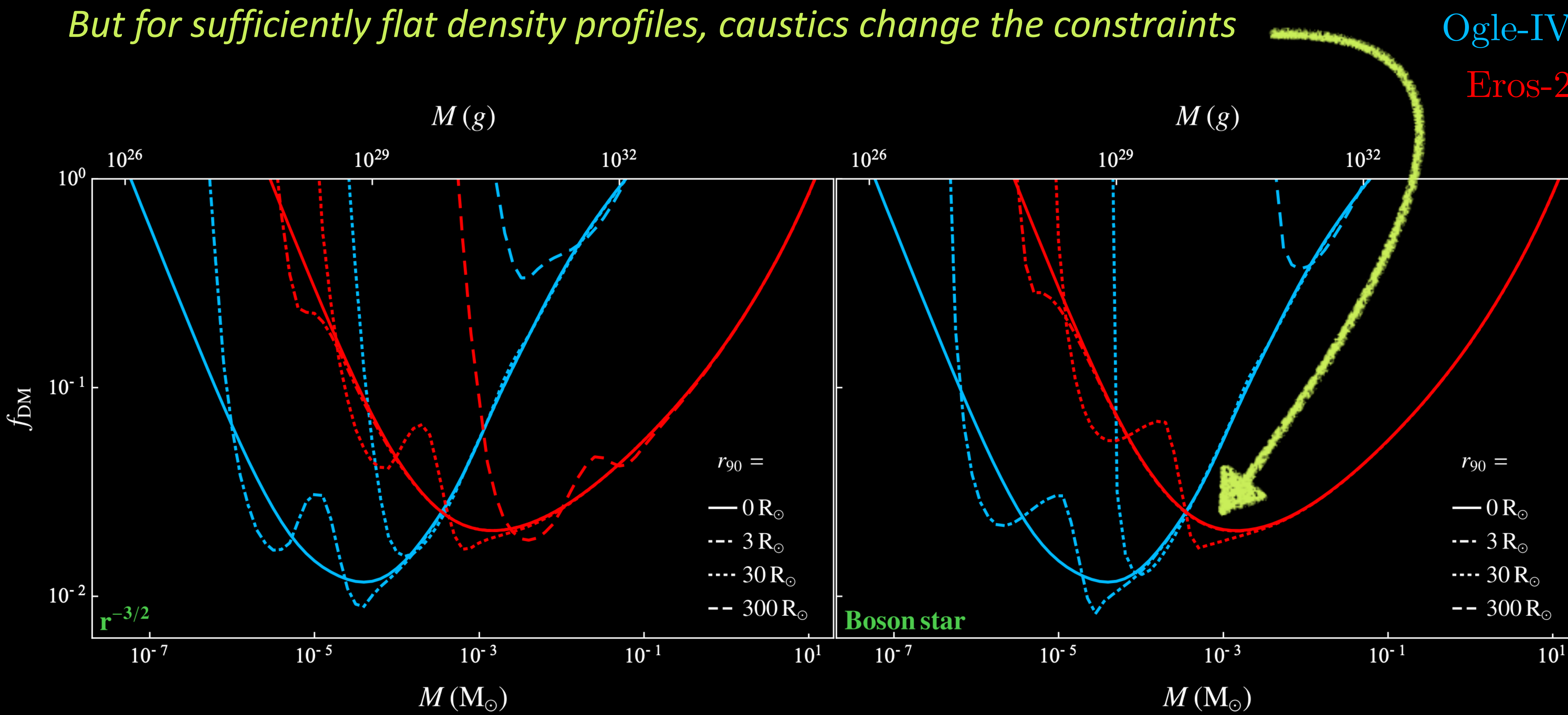

DC, D. McKeen, N. Raj, PRD, arXiv:2002.08962 [astro-ph.CO]

DC, D. McKeen, N. Raj, Z. Wang, PRD, arXiv:2007.12697 [astro-ph.CO]

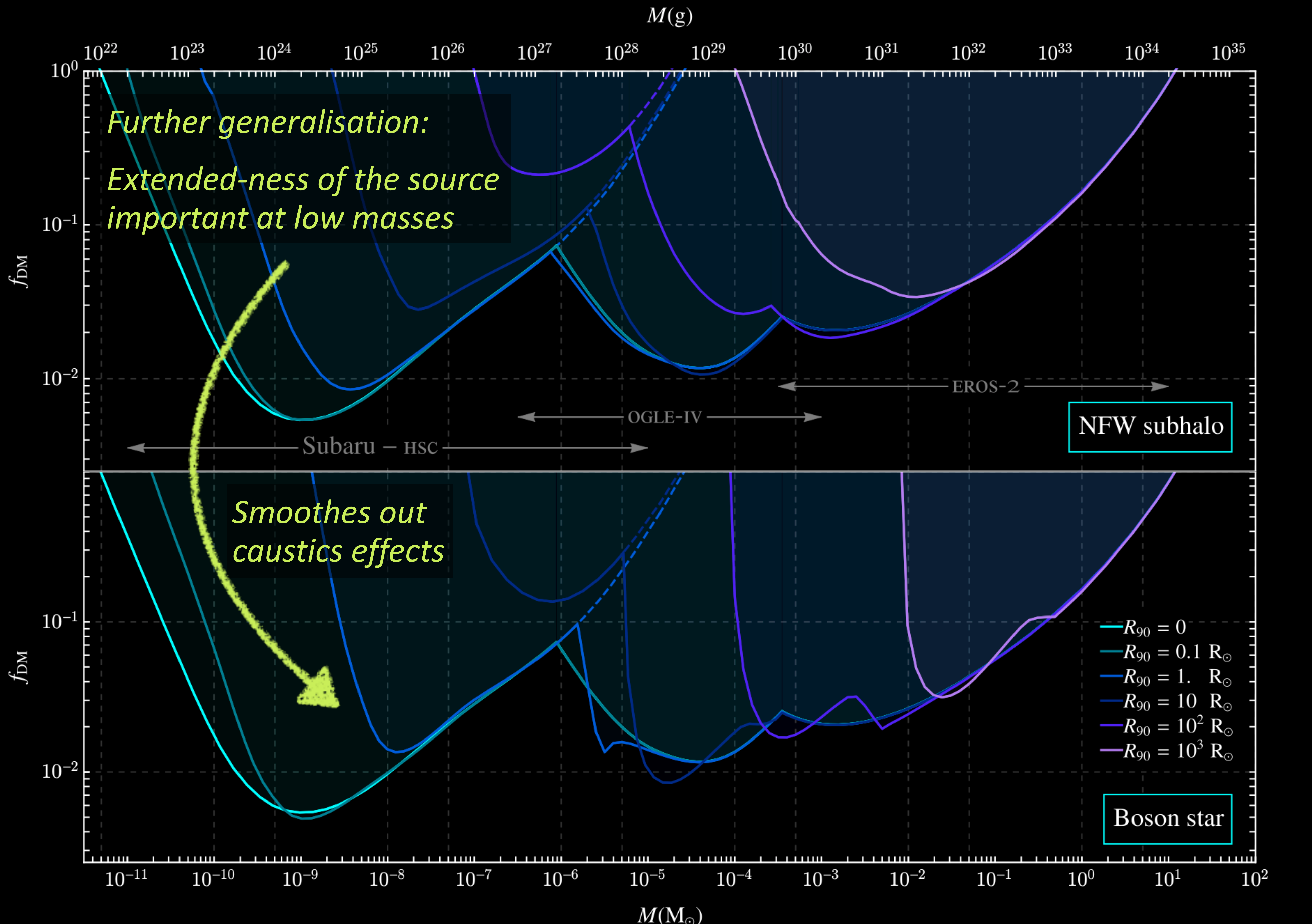

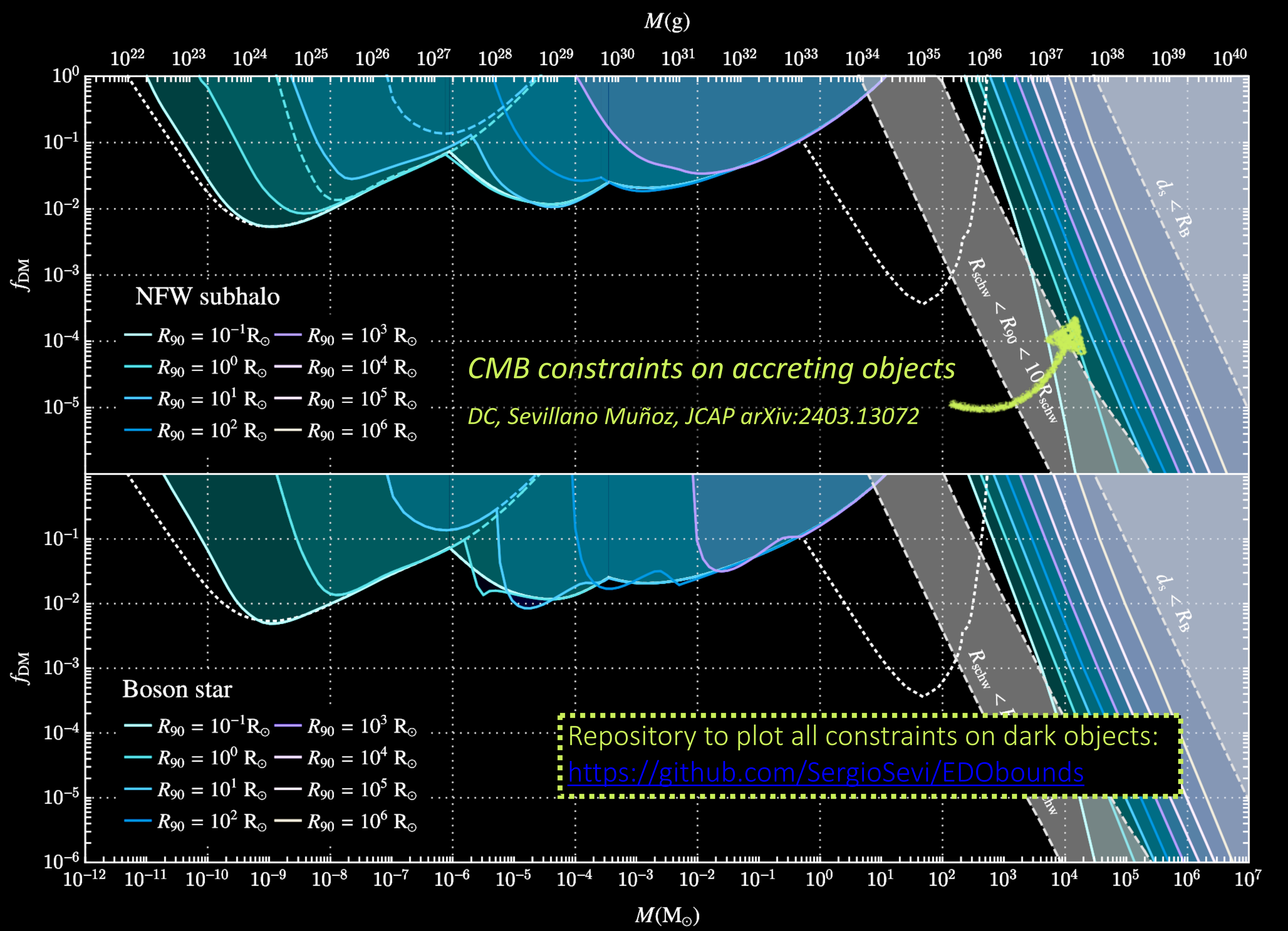

M(g)
10^{22} 10^{23} 10^{24} 10^{25} 10^{26} 10^{27} 10^{28} 10^{29} 10^{30} 10^{31} 10^{32} 10^{33} 10^{34} 10^{35} 10^{36} 10^{37} 10^{38} 10^{39} 10^{40}
f_{DM}
10^{0} 10^{-1} 10^{-2} 10^{-3} 10^{-4} 10^{-5}
NFW subhalo
$R_{90} = 10^{-1} R_\odot$
$R_{90} = 10^{0} R_\odot$
$R_{90} = 10^{1} R_\odot$
$R_{90} = 10^{2} R_\odot$
$R_{90} = 10^{3} R_\odot$
$R_{90} = 10^{4} R_\odot$
$R_{90} = 10^{5} R_\odot$
$R_{90} = 10^{6} R_\odot$
CMB constraints on accreting objects
DC, Sevillano Muñoz, JCAP arXiv:2403.13072
$R_{schw} < R_{90} < 10 R_{schw}$
$d_s < R_B$
f_{DM}
10^{-1} 10^{-2} 10^{-3} 10^{-4} 10^{-5} 10^{-6}
Boson star
$R_{90} = 10^{-1} R_\odot$
$R_{90} = 10^{0} R_\odot$
$R_{90} = 10^{1} R_\odot$
$R_{90} = 10^{2} R_\odot$
$R_{90} = 10^{3} R_\odot$
$R_{90} = 10^{4} R_\odot$
$R_{90} = 10^{5} R_\odot$
$R_{90} = 10^{6} R_\odot$
Repository to plot all constraints on dark objects:
https://github.com/SergioSevi/EDObounds
$d_s < R_B$
10^{-12} 10^{-11} 10^{-10} 10^{-9} 10^{-8} 10^{-7} 10^{-6} 10^{-5} 10^{-4} 10^{-3} 10^{-2} 10^{-1} 10^{0} 10^{1} 10^{2} 10^{3} 10^{4} 10^{5} 10^{6} 10^{7}
$M(M_\odot)$

Light curves with caustics

Can we look for these explicitly?

M. Crispim-Romao, DC, PRD, arXiv:2402.00107

Preview with OGLE-II timestamps

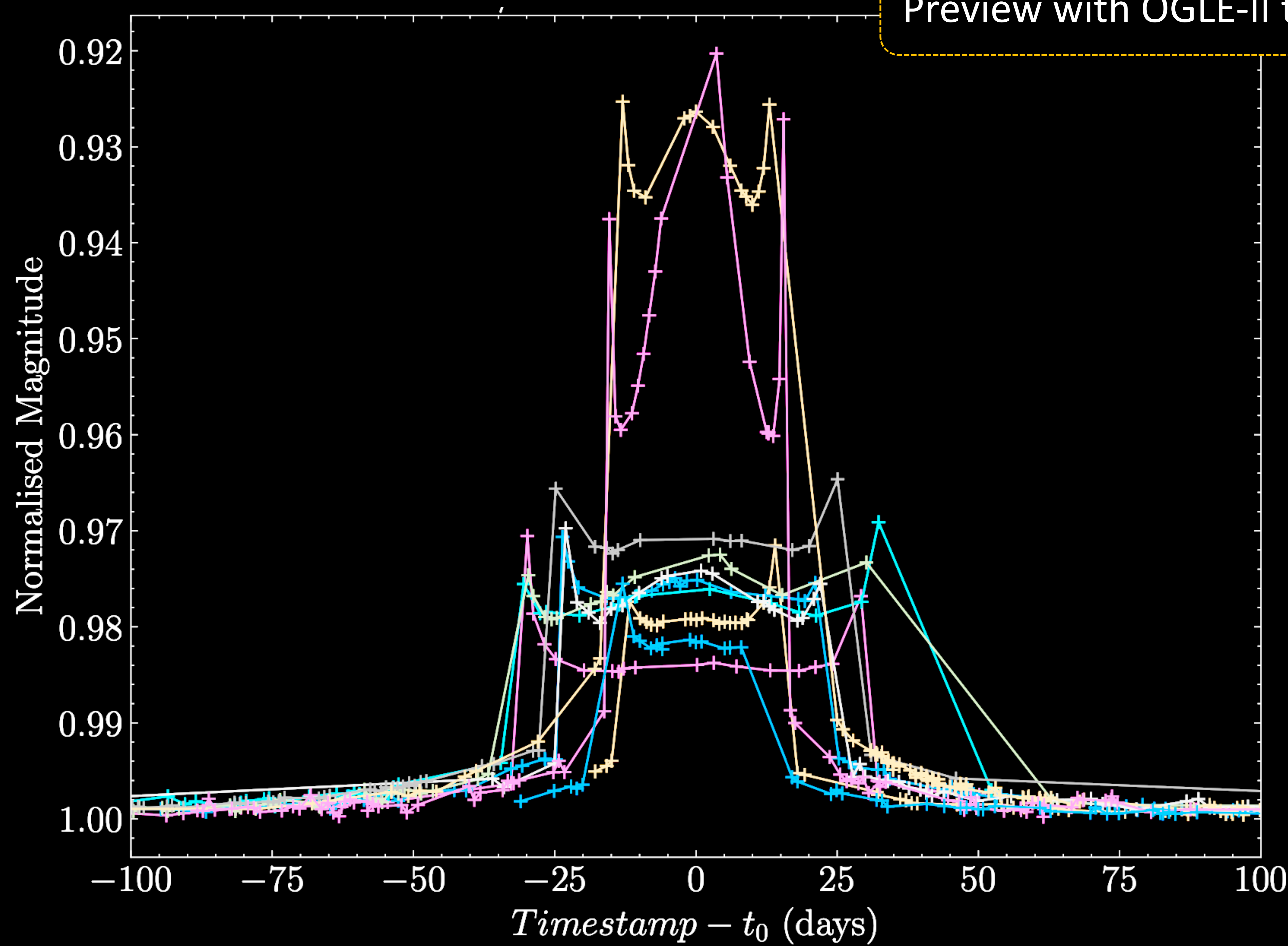

Miguel Crispim-Romao, DC, PRD, arXiv:2402.00107

ML + ML

Microlensing + Machine Learning

- Microlensing data is time series data
- Challenge: low-cadence data, lower signal-to-noise ratios

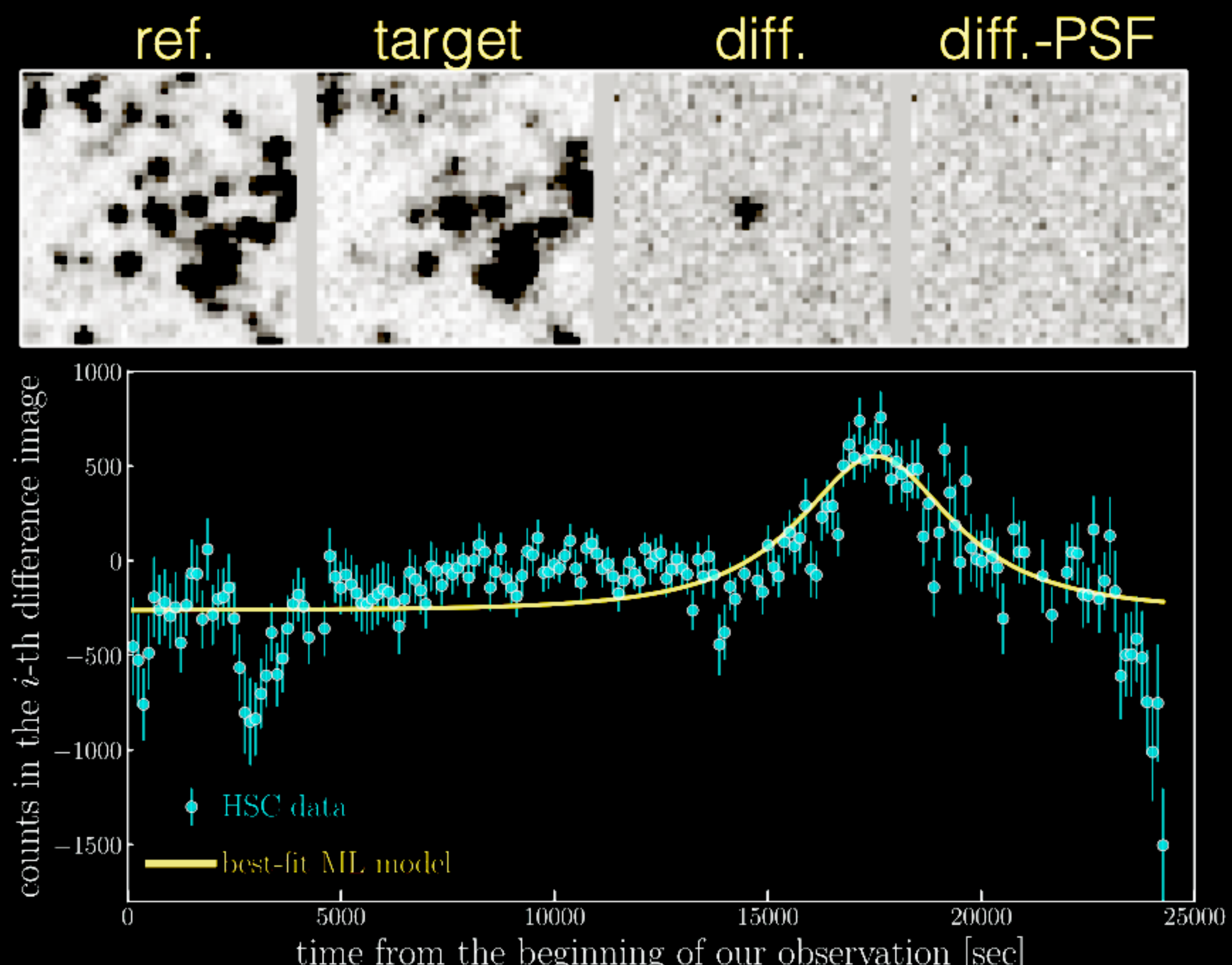

From the Subaru collaboration, arXiv:1701.02151

Miguel Crispim-Romao, DC, PRD, arXiv:2402.00107

ML + ML

Microlensing + Machine Learning

- Microlensing data is time series data
- Challenge: low-cadence data, lower signal-to-noise ratios
- MicroLIA: use a Random Forest (RF) algorithm to find microlensing event (and distinguish from other events)

Godines et al, arXiv:2004.14347

Miguel Crispim-Romao, DC, PRD, arXiv:2402.00107

ML + ML

Microlensing + Machine Learning

- Microlensing data is time series data
- Challenge: low-cadence data, lower signal-to-noise ratios
- MicroLIA: use a Random Forest (RF) algorithm to find microlensing event (and distinguish from other events)

Our adaptations:

- Implement boson star and NFW light curves with $0.5 < \tau_m < 5$
- Instead of an RF, we use a histogram-based gradient boosted classifier (HBGC) to improve speed
- Add criterium $\mu \geq 1.34$

(… and a few fixes)

Complete datasets not available

Table 1
Selection Criteria for High-quality Microlensing Events in OGLE GVS Fields

Criteria	Remarks	Number
All stars in databases		1,856,529,265
$\chi^2_{\rm out}/{\rm dof} \leqslant 2.0$	No variability outside a window centered on the event (duration of the window depends on the field)	
$n_{\rm DIA} \geqslant 3$	Centroid of the additional flux coincides with the source star centroid	
$\chi_{3+} = \sum_i (F_i - F_{\rm base})/\sigma_i \geqslant 32$	Significance of the bump	23,618
$A \geqslant 0.1$ mag	Rejecting low-amplitude variables	
$n_{\rm bump} = 1$	Rejecting objects with multiple bumps	18,397
	Fit quality:	
$\chi^2_{\rm fit}/{\rm dof} \leqslant 2.0$	χ^2 for all data	
$\chi^2_{{\rm fit},t{\rm E}}/{\rm dof} \leqslant 2.0$	χ^2 for $\|t - t_0\| < t_{\rm E}$	
$\sigma(t_{\rm E})/t_{\rm E} < 0.5$	Einstein timescale is well measured	
$t_{\rm min} \leqslant t_0 \leqslant t_{\rm max}$	Event peaked between $t_{\rm min}$ and $t_{\rm max}$, which are moments of the first and last observation of a given field	
$u_0 \leqslant 1$	Maximum impact parameter	
$t_{\rm E} \leqslant 500$ d	Maximum timescale	
$A \geqslant 0.4$ mag if $t_{\rm E} \geqslant 100$ days	Long-timescale events should have high amplitudes	
$I_{\rm s} \leqslant 21.0$	Maximum I-band source magnitude	
$F_{\rm b} > -F_{\rm min}$	Maximum negative blend flux, corresponding to $I = 20.5$ mag star	460

Reject events with multiple bumps

So for now… generating and injecting events

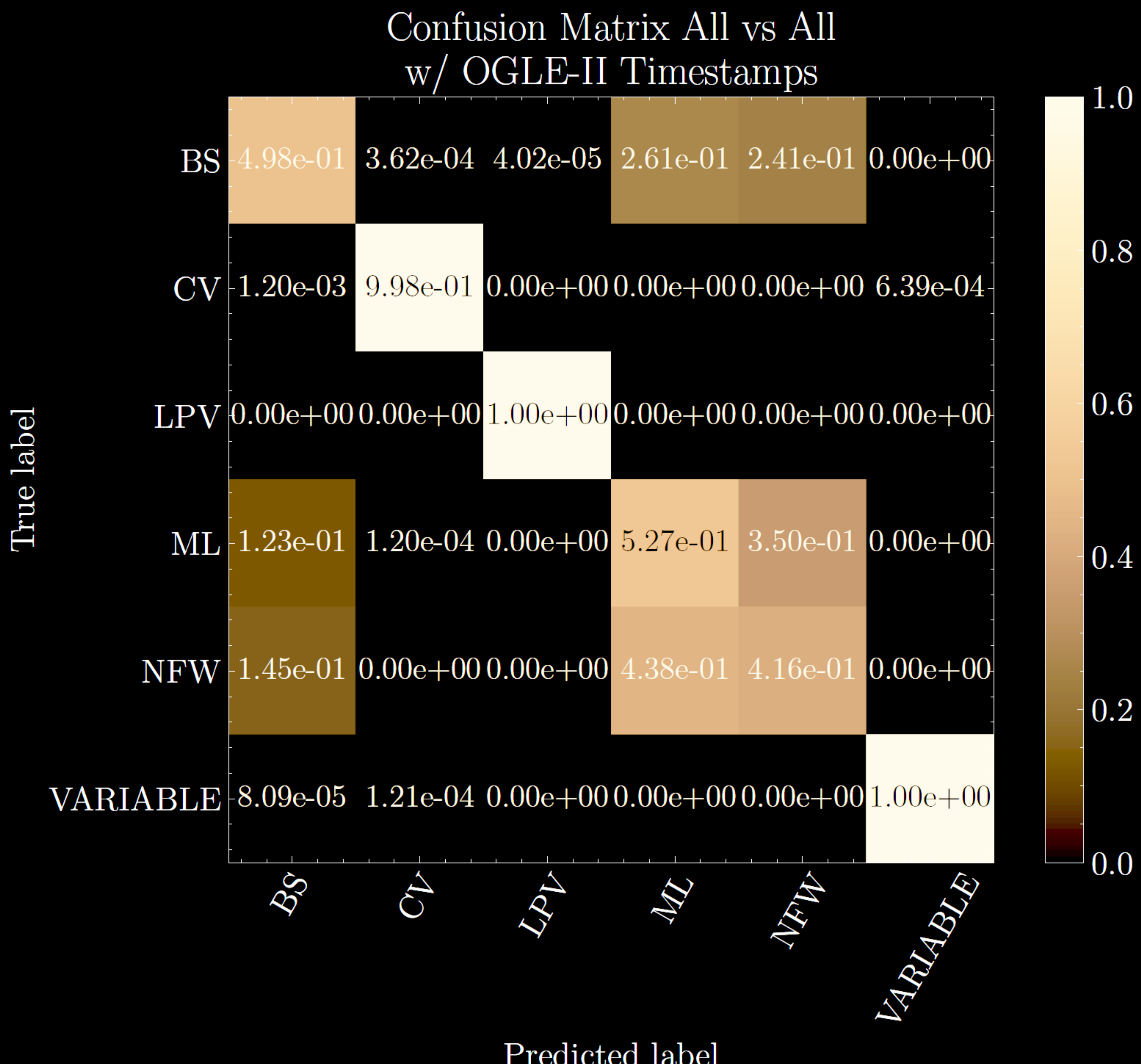

Miguel Crispim-Romao, DC, arXiv:2402.00107

Confusion Matrix All vs All
w/ OGLE-II Timestamps

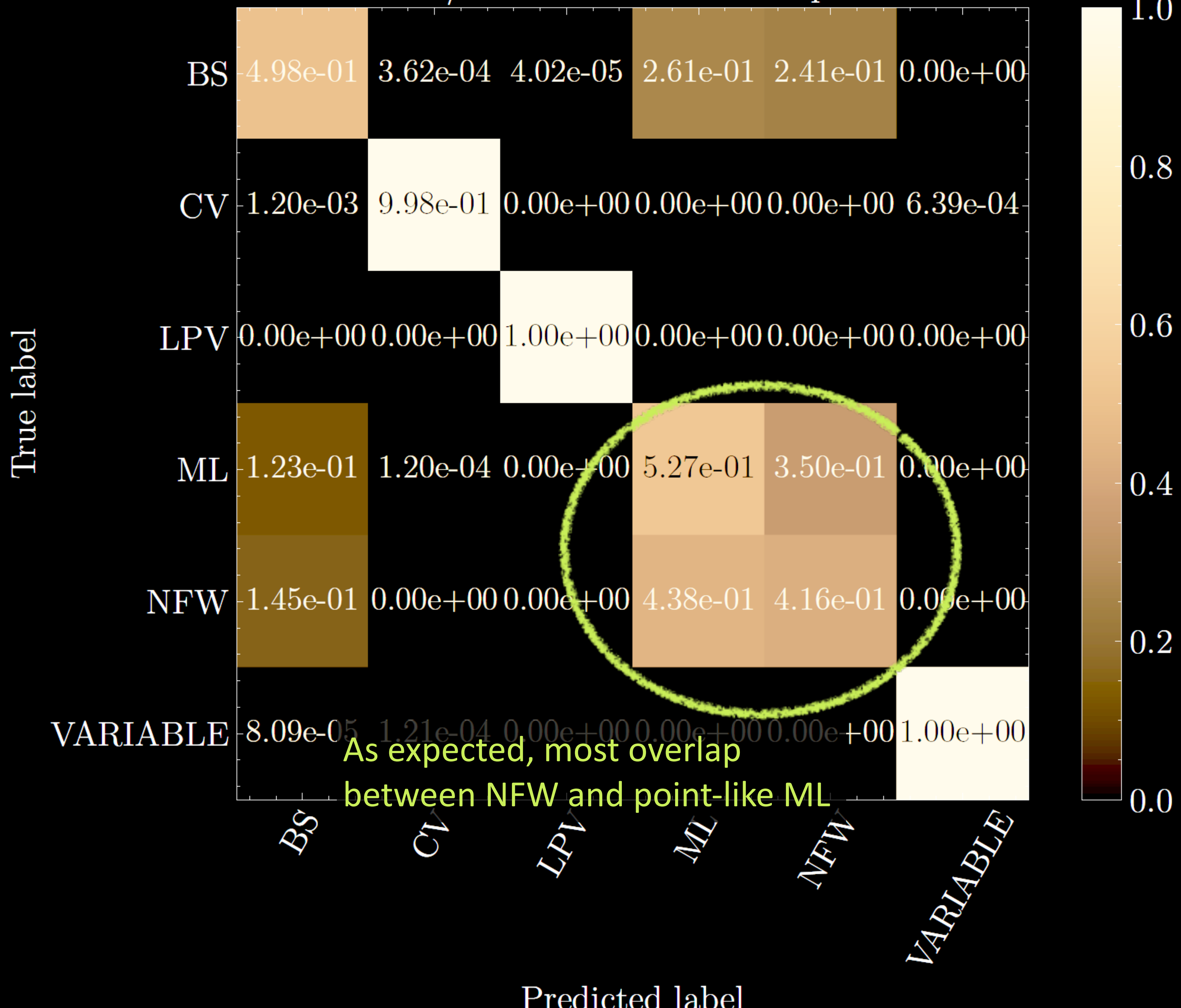

Miguel Crispim-Romao, DC, arXiv:2402.00107

Miguel Crispim-Romao, DC, PRD, arXiv:2402.00107

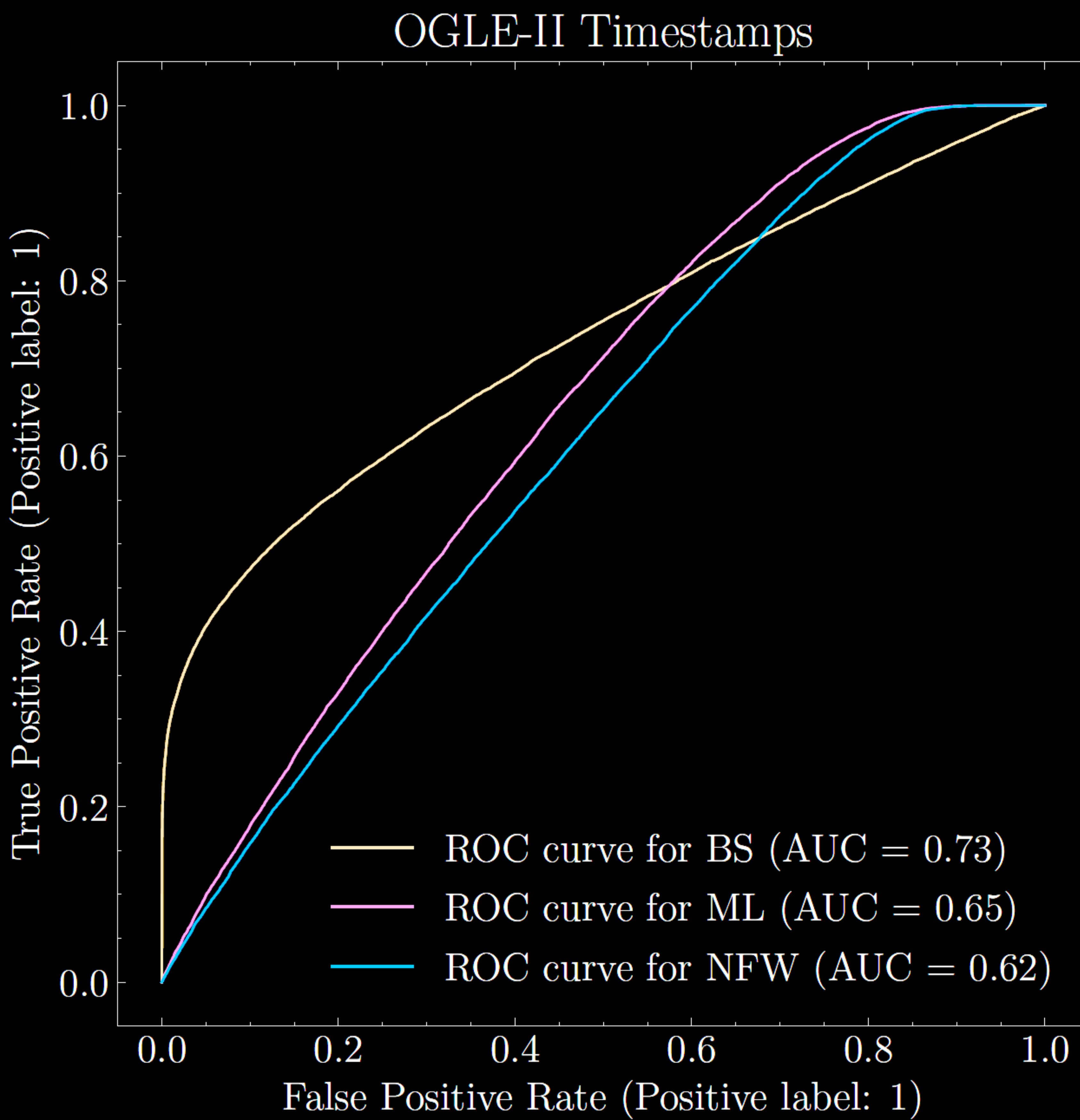

Miguel Crispim-Romao, DC, PRD, arXiv:2402.00107

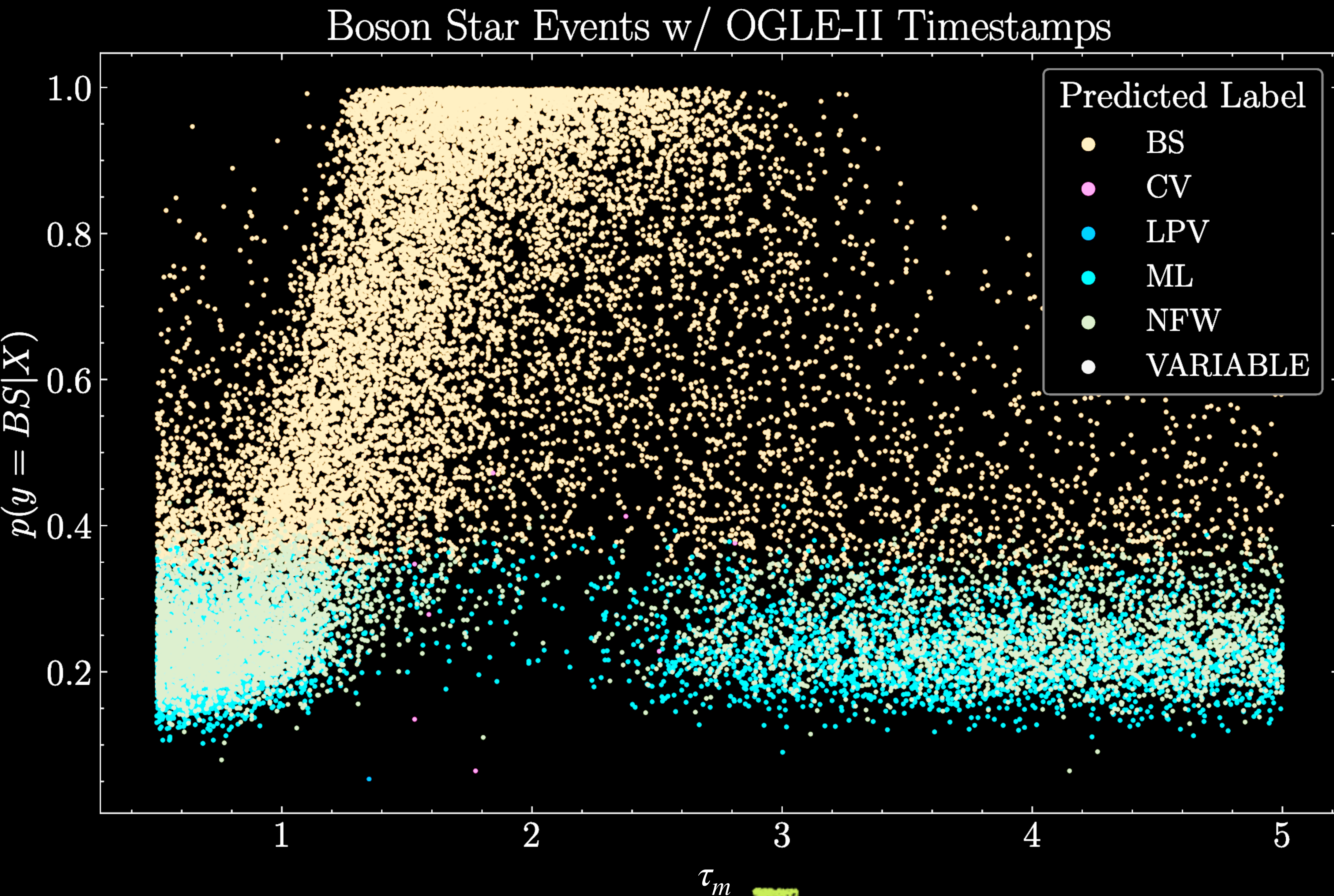

$$\tau_m \equiv \theta_{\text{lens}}/\theta_E = r_{\text{lens}}/r_E$$

Miguel Crispim-Romao, DC, PRD, arXiv:2402.00107

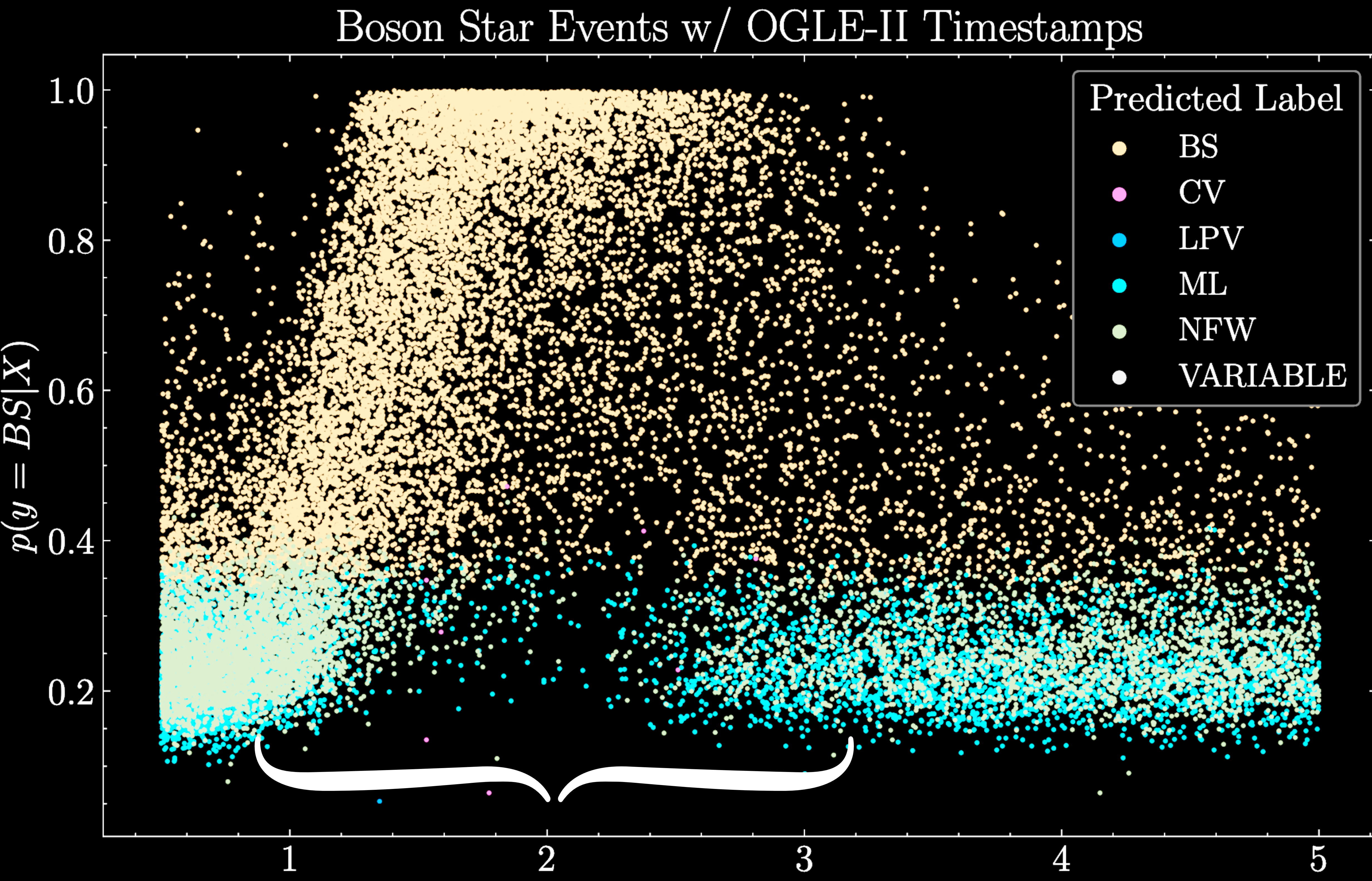

Indeed, the most probable detections are for $0.8 < \tau_m < 3$

$$\tau_m \equiv \theta_{\text{lens}}/\theta_E = r_{\text{lens}}/r_E$$

LSST by Rubin

The Legacy Survey of Space and Time

- 10-year survey by the Vera C. Rubin Observatory
- Large field of view and rapid survey speed
- Relatively high cadence observations, allowing frequent monitoring of $\sim 10^9$ stars
- However, sparse — *develop follow up strategies*

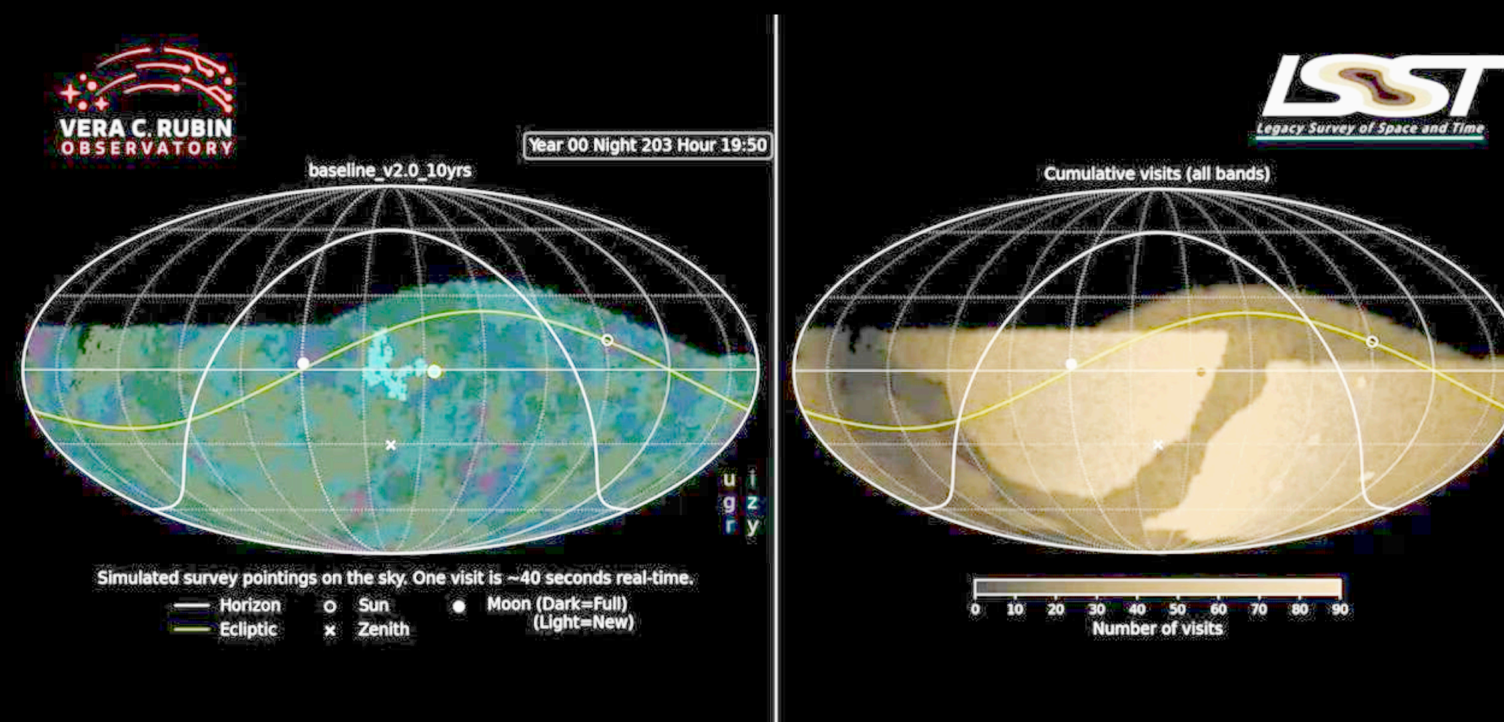

LSST by Rubin: simulations

https://zenodo.org/records/15005108

Miguel Crispim-Romao, DC, Daniel Godines, arXiv:2503.09699

Simulated, using rubinsim, 7 classes of observations:

- *Constant*
- Mira long-period variables (LPV)
- RR Lyrae and Cepheid Variables (RRLyrae)
- point-like microlensing (ML)
- binary microlensing
- microlensing by NFW-subhalos
- microlensing by boson stars (BS)

Cadence: (`baseline_v2.0_10yrs`)

parameter	min	max	spacing
t_E (days)	0	100	linear
u_0	0	3	linear
τ_m	0.05	5	logarithmic

LSST by Rubin: anomaly detection

Miguel Crispim-Romao, DC, Daniel Godines, arXiv:2503.09699

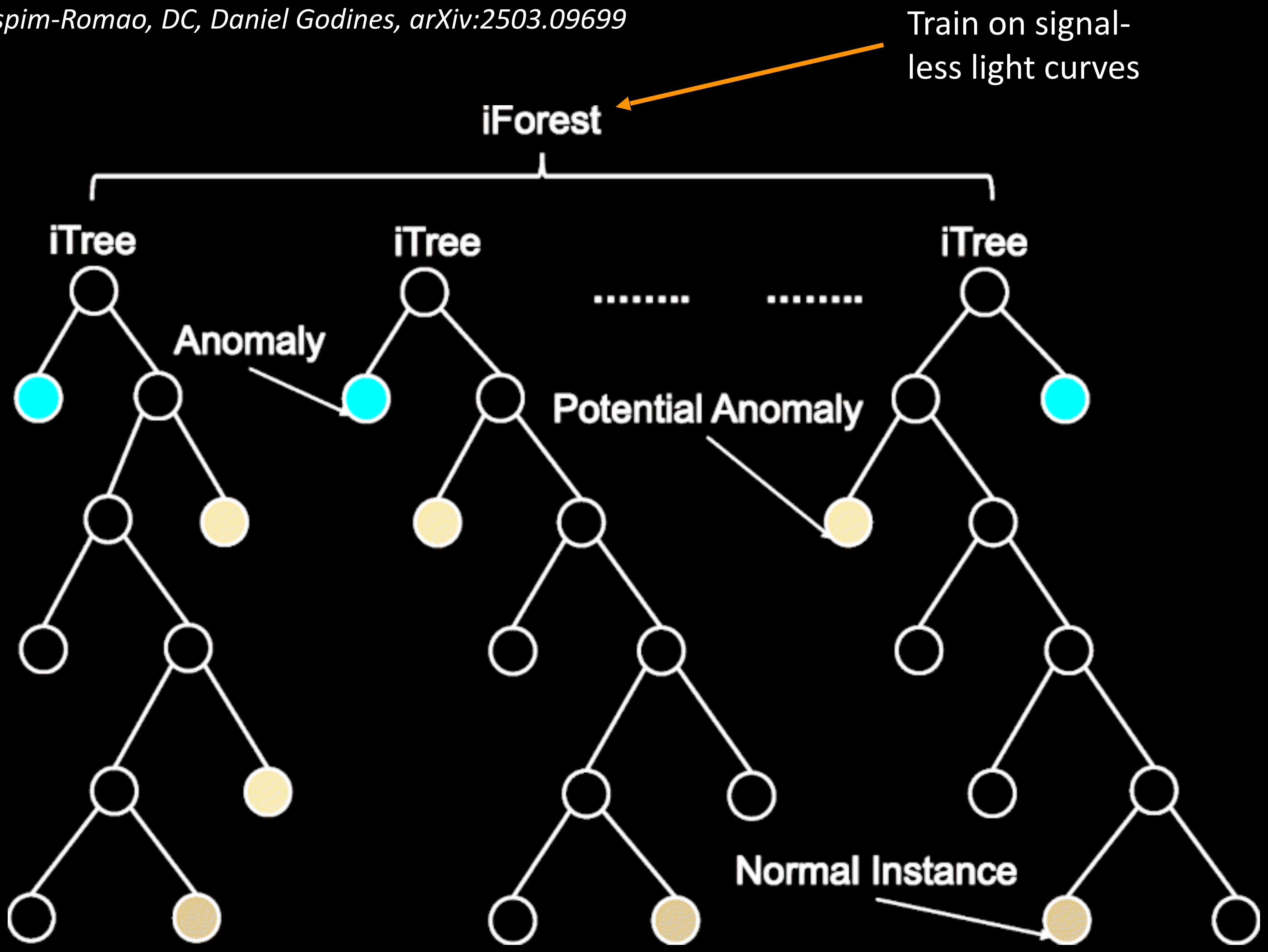

LSST by Rubin: offline analysis

Miguel Crispim-Romao, DC, Daniel Godines, arXiv:2503.09699

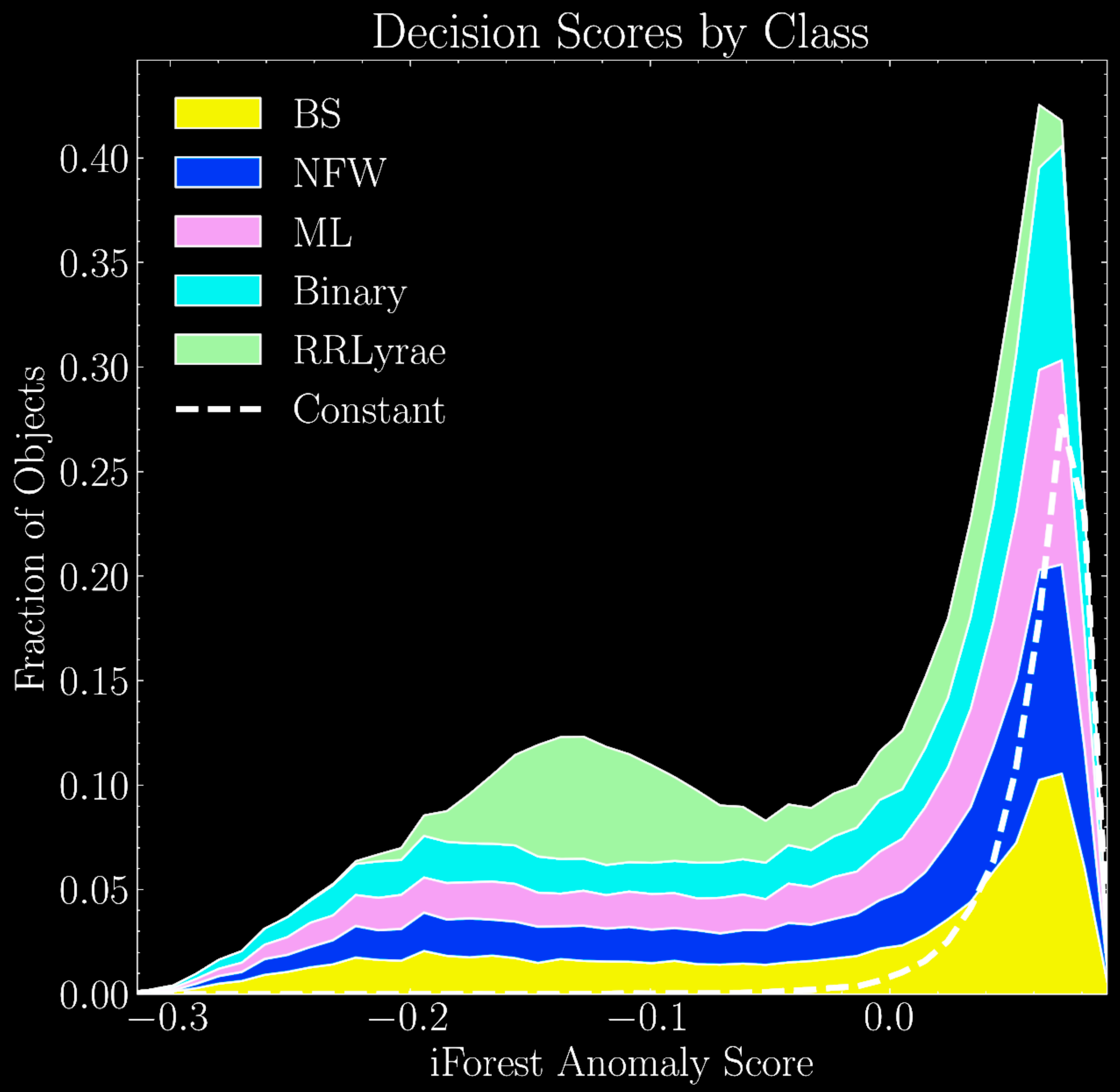

LSST by Rubin: offline analysis

Miguel Crispim-Romao, DC, Daniel Godines, arXiv:2503.09699

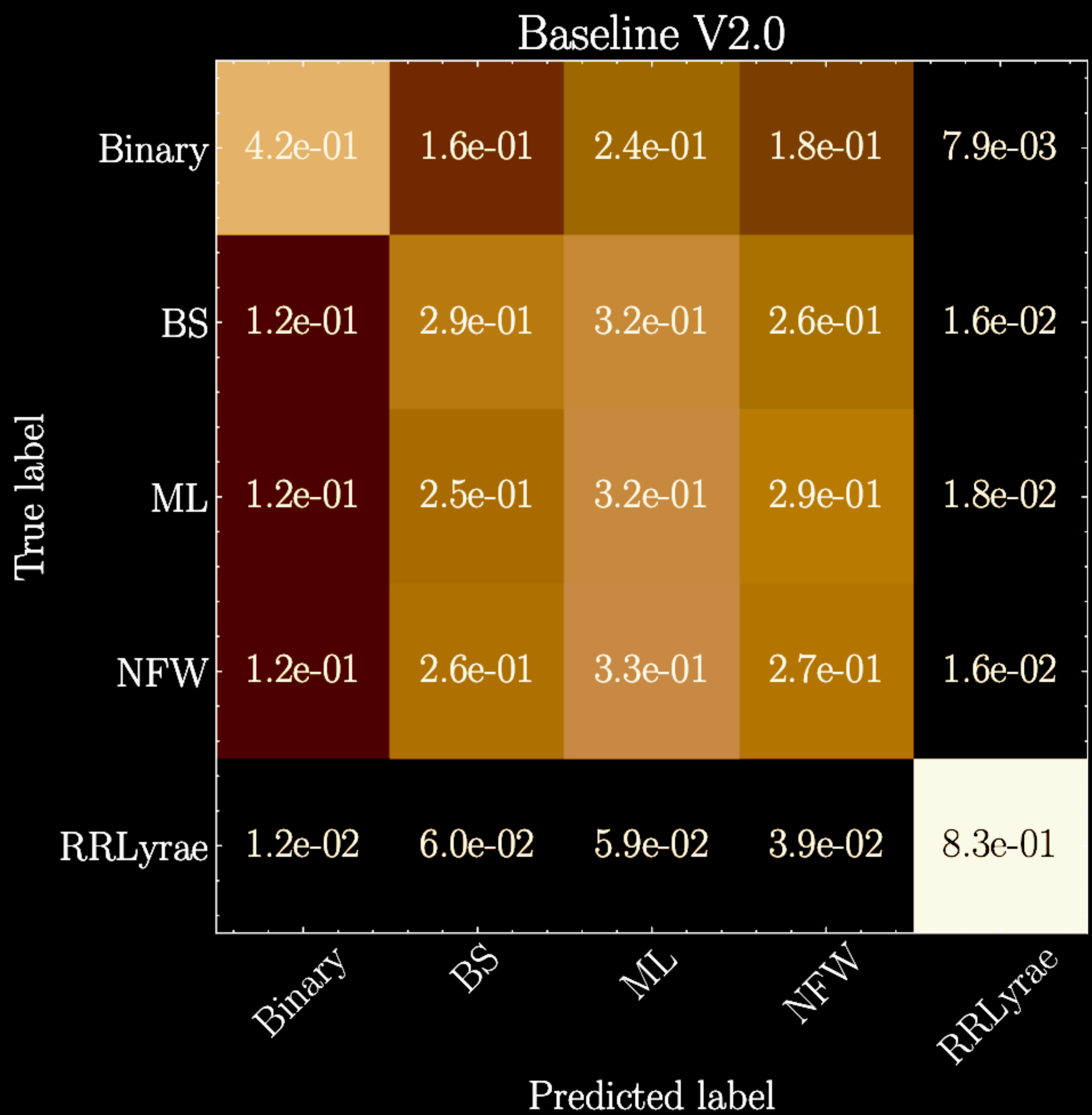

LSST by Rubin: online analysis

Miguel Crispim-Romao, DC, Daniel Godines, arXiv:2503.09699

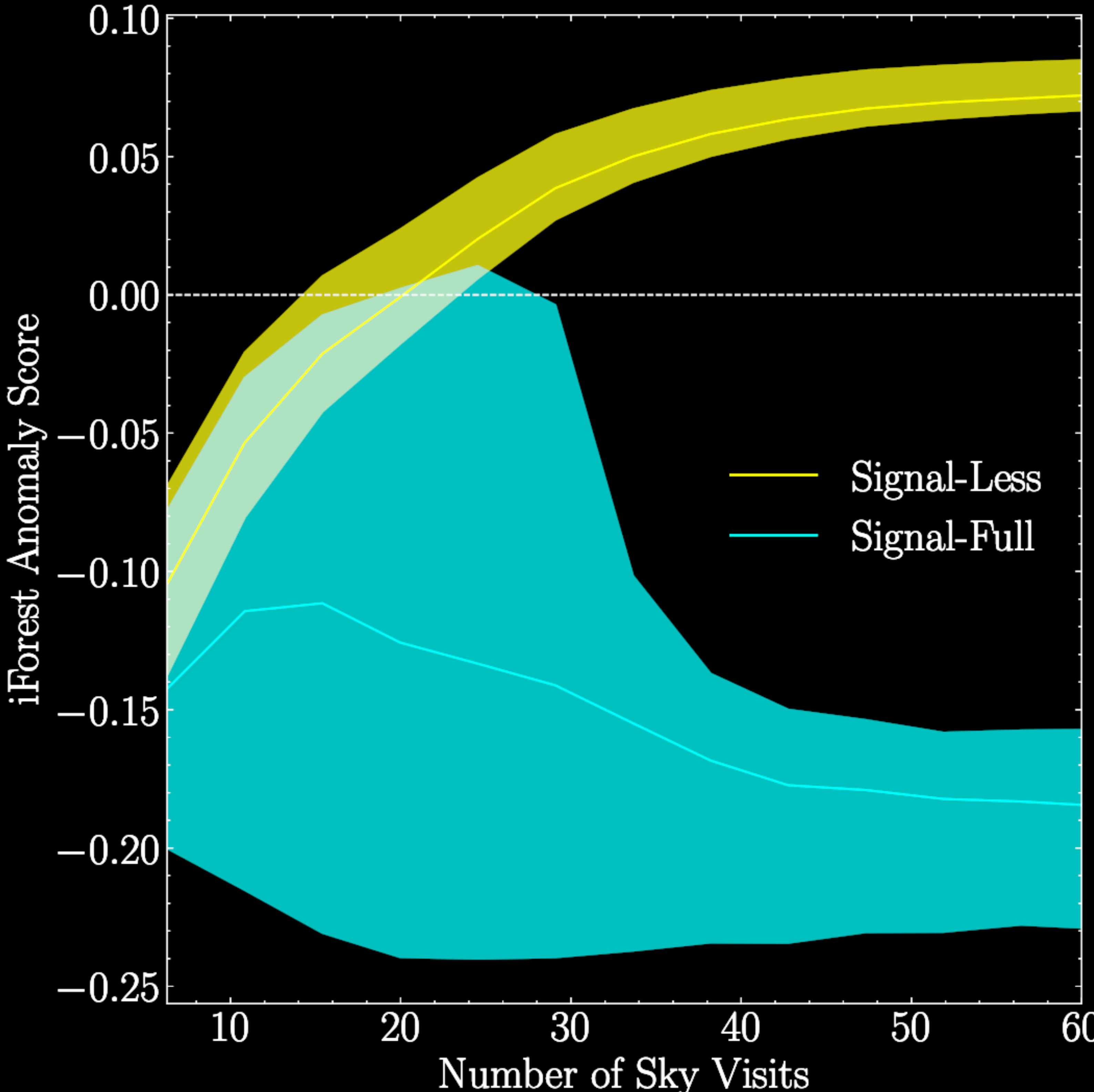

LSST by Rubin: projections

Miguel Crispim-Romao, DC, Benedict Crossey, Daniel Godines, arXiv:2506.XXXX

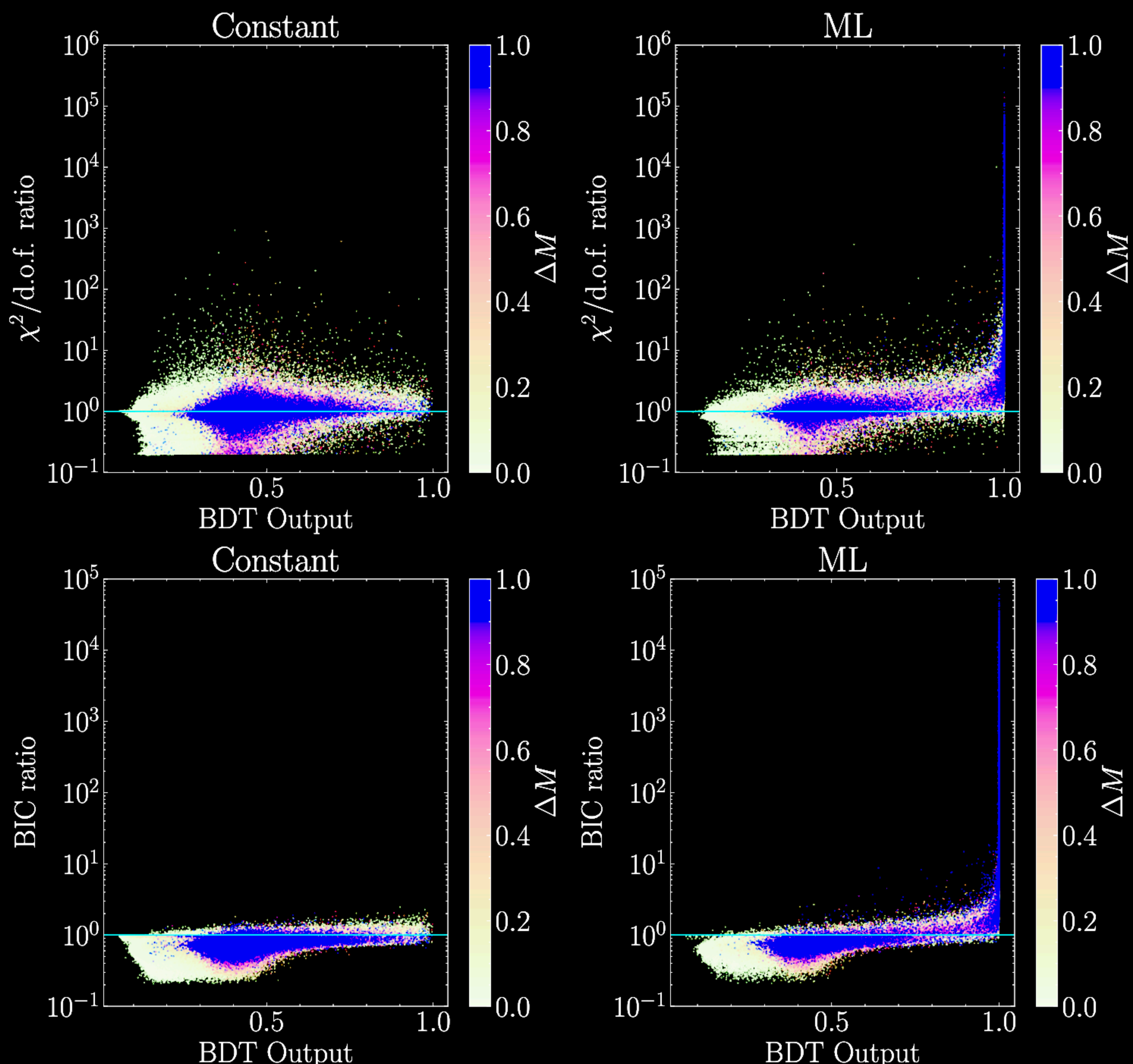

LSST by Rubin: projections

Miguel Crispim-Romao, DC, Benedict Crossey, Daniel Godines, arXiv:2506.XXXX

Goal: design cuts which optimise efficiency while minimising false positives

Typically used

BIC

BDT

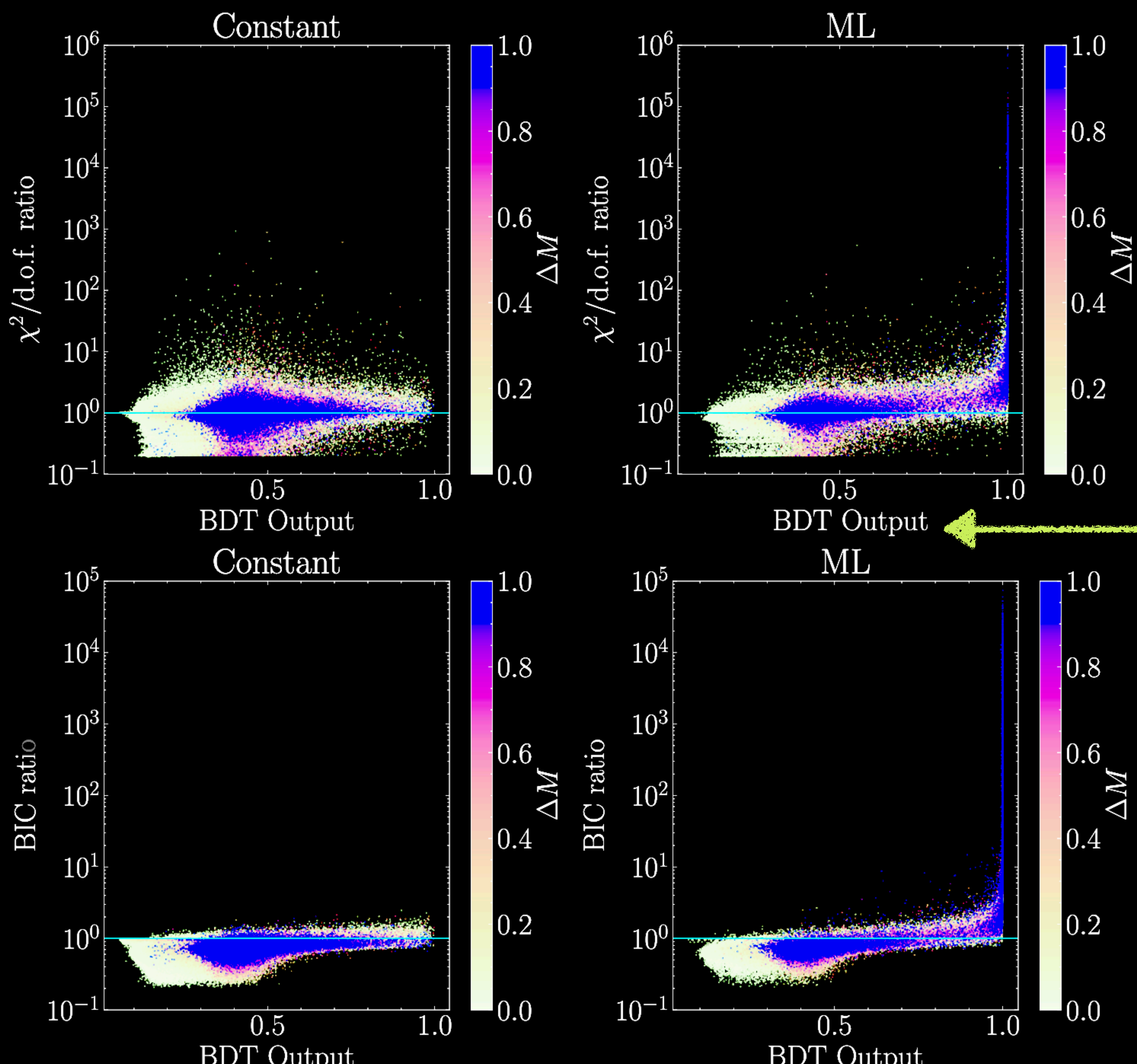

LSST by Rubin: projections

Miguel Crispim-Romao, DC, Benedict Crossey, Daniel Godines, arXiv:2506.XXXX

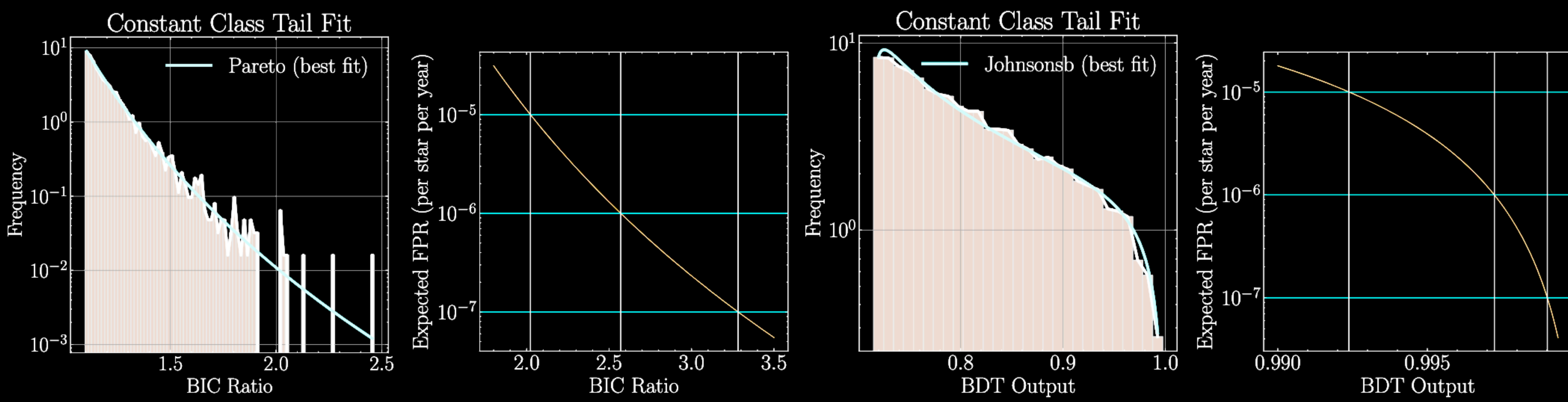

For competitive constraints, need FPR $< 10^{-7}$

cut	FPR	$\bar{\epsilon}$
BIC ratio > 3.28	10^{-7}	0.38
BDT > 0.999	10^{-7}	0.34
χ^2/d.o.f. ratio > 10	3.5×10^{-4}	0.30
χ^2/d.o.f. ratio > 10, $\tilde{u}_0 < 1$	1.1×10^{-4}	0.20

LSST by Rubin: projections

Miguel Crispim-Romao, DC, Benedict Crossey, Daniel Godines, arXiv:2506.XXXX

Define a cut in false positives — what fraction of events is identified?

$$\epsilon \equiv N_{>\mathrm{cut}}/N_{\mathrm{total}}$$

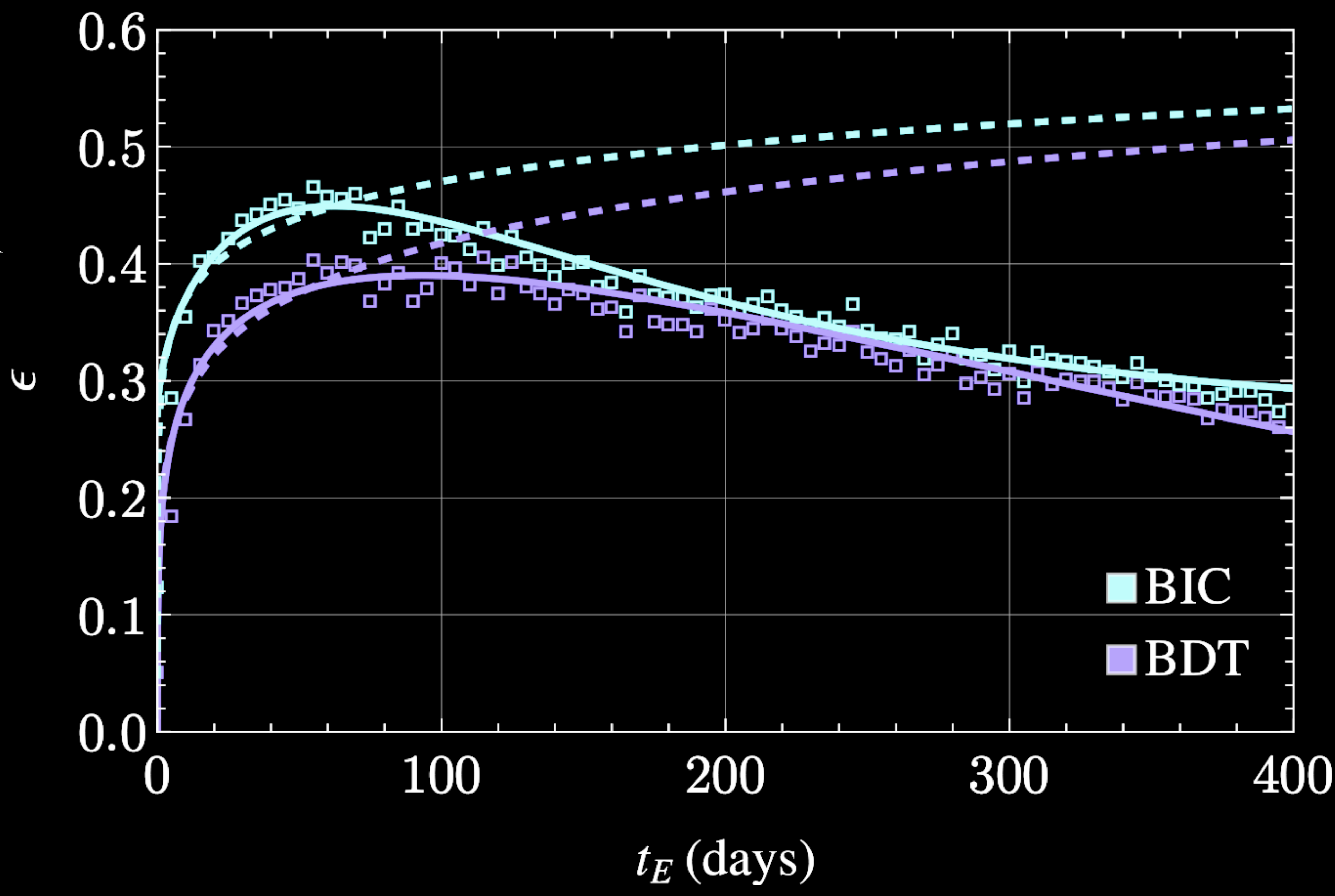

LSST by Rubin: projections

Miguel Crispim-Romao, DC, Benedict Crossey, Daniel Godines, arXiv:2506.XXXX

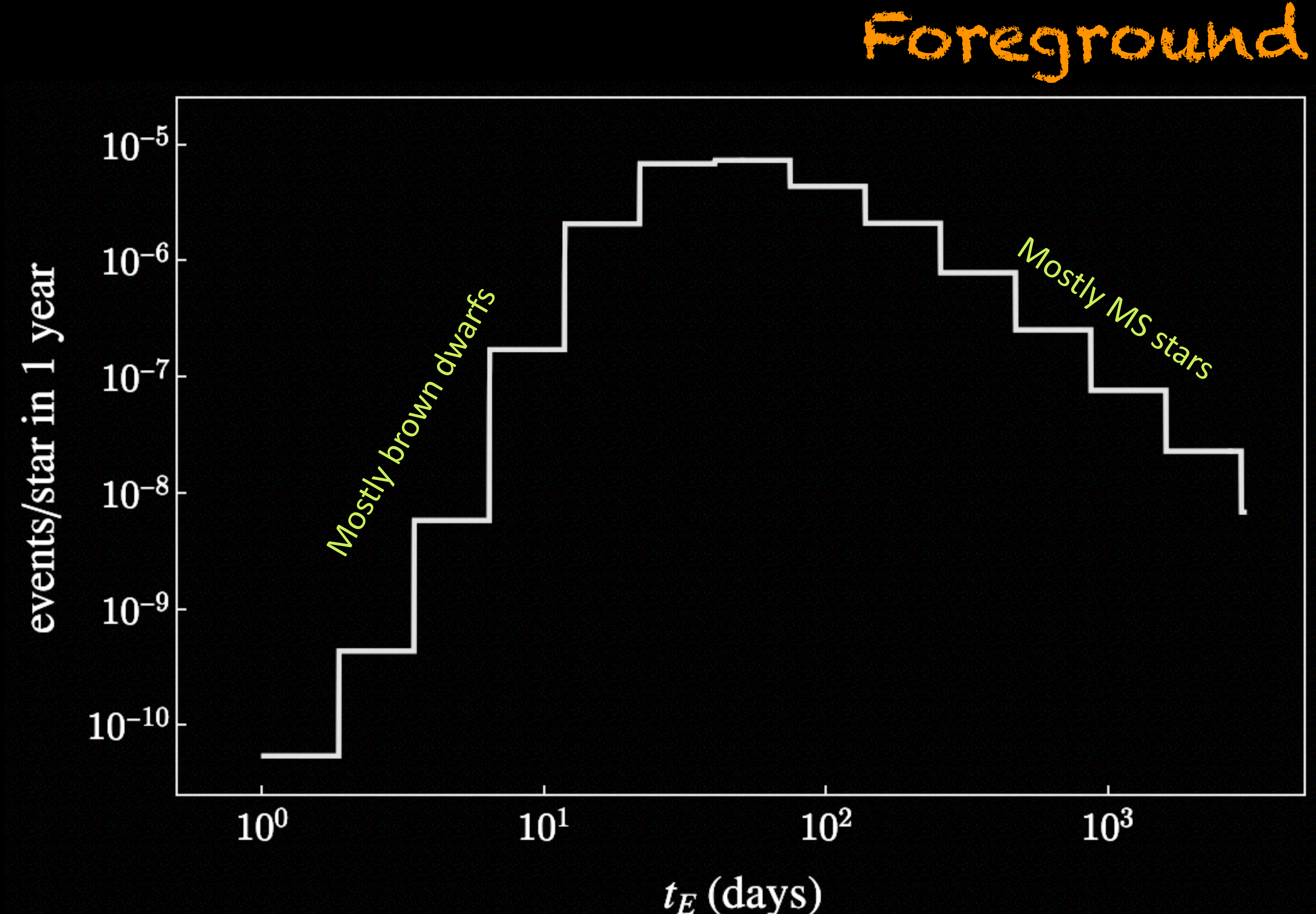

LSST by Rubin: projections

Miguel Crispim-Romao, DC, Benedict Crossey, Daniel Godines, arXiv:2506.XXXX

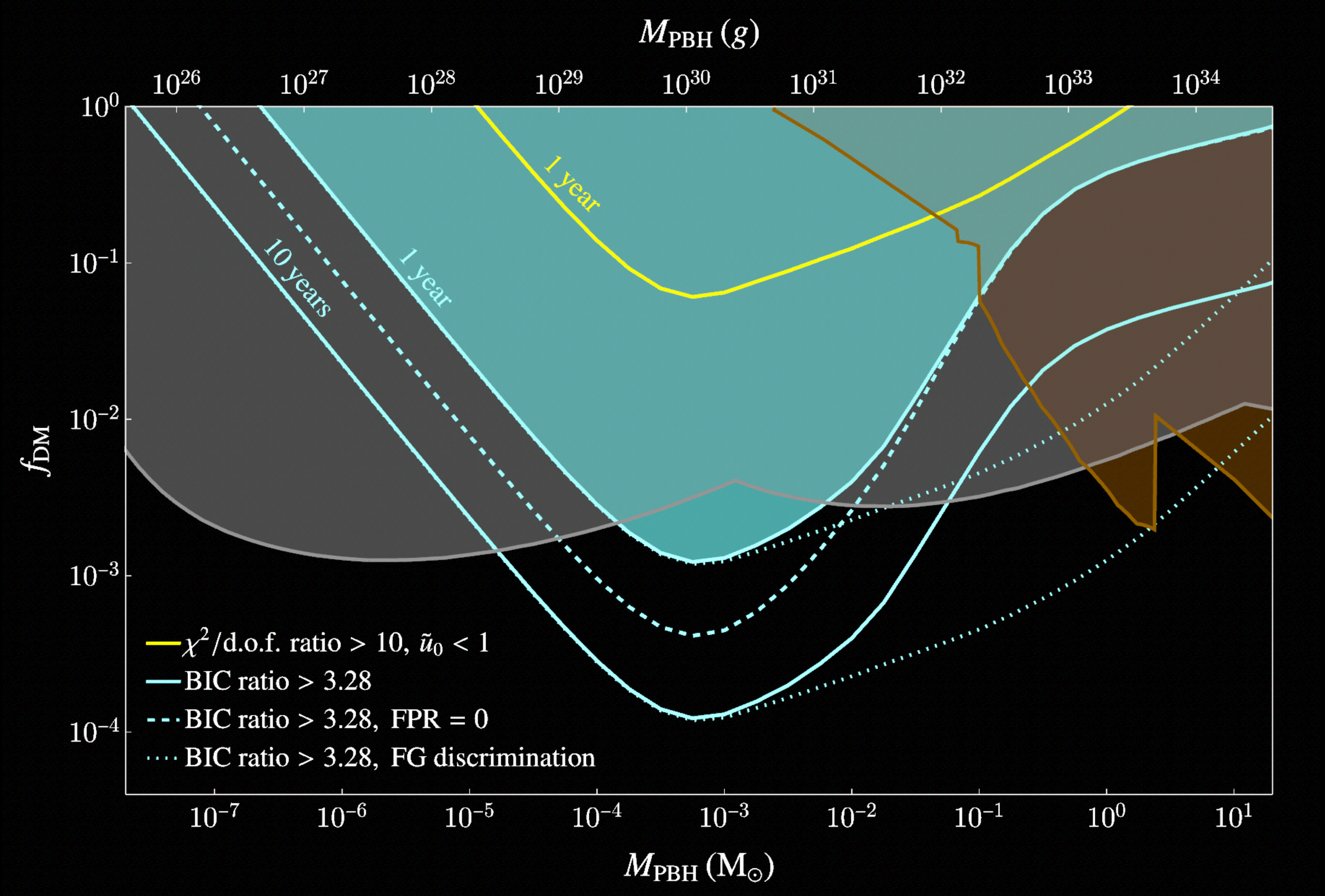

Bringmann, DC, Sevillano Muñoz, arXiv:2506.XXXX

EDOs and the early Universe

- Ultracompact mini haloes (UCMH, $\rho \sim r^{-3/2}$) are formed from the collapse of primordial overdensities

- The non-observation of UCMH can therefore be used to draw conclusions about the primordial power spectrum

- This has been done for e.g. PTAs and WIMPs (= model-dependent)

Clark, Lewis, Scott, MNRAS, arXiv:1509.02938
Bringmann, Scott, Akrami, PRD, arXiv:1110.2484

- But we now have far more gravitational probes…

Bringmann, DC, Sevillano Muñoz, arXiv:2506.XXXX

The primordial power spectrum

- Primordial curvature perturbations with amplitude $\mathscr{P}_{\mathscr{R}}(k)$ determine the variance $\sigma_{\chi,H}(R)$ of CDM density fluctuations at horizon entry
  - If $\delta_\chi(R)$ exceeds a threshold $\delta_\chi^{\min}(R) \sim 10^{-3}$, the region collapses into an UCMH (much smaller than for PBHs)
  - If $\sigma_{\chi,H}(R)$ is too large many regions will exceed $\delta_\chi^{\min}(R)$

Bringmann, DC, Sevillano Muñoz, arXiv:2506.XXXX

The primordial power spectrum

- Primordial curvature perturbations with amplitude $\mathscr{P}_{\mathscr{R}}(k)$ determine the variance $\sigma_{\chi,H}(R)$ of CDM density fluctuations at horizon entry
  - If $\delta_\chi(R)$ exceeds a threshold $\delta_\chi^{\rm min}(R) \sim 10^{-3}$, the region collapses into an UCMH
  - If $\sigma_{\chi,H}(R)$ is too large many regions will exceed $\delta_\chi^{\rm min}(R)$
- From $f_{\rm DM}$ we work backward:
  - $f_{\rm DM}$ sets a max collapse probability $\beta_{max}(R)$ at redshift z_c
  - In Gaussian theory, $\beta(R) \sim \exp[-\delta_{min}^2/(2\sigma^2(R))]$. Thus β_{max} fixes the largest allowable $\sigma(R)$
  - Since $\sigma^2(R)$ is essentially an integral over $\mathscr{P}_{\mathscr{R}}(k)$ around $k \sim 1/R$, limiting $\sigma(R) \Rightarrow$ upper limit on $\mathscr{P}_{\mathscr{R}}(k)$

Bringmann, DC, Sevillano Muñoz, arXiv:2506.XXXX

The primordial power spectrum

- Assume a generalised power spectrum

- EDOs formed with

$$\frac{R(z_c)}{\mathrm{pc}} = 0.019\left(\frac{1000}{z_c+1}\right)\left(\frac{M(z_c)}{M_\odot}\right)^{1/3} \text{ with } M(z_c) = \frac{z_{\mathrm{eq}}+1}{z_c+1}M_i$$

Bringmann, DC, Sevillano Muñoz, arXiv:2506.XXXX

The primordial power spectrum

- Assume a generalised power spectrum

- EDOs formed with

$$\frac{R(z_c)}{\mathrm{pc}} = 0.019\left(\frac{1000}{z_c+1}\right)\left(\frac{M(z_c)}{M_\odot}\right)^{1/3} \quad \text{with } M(z_c) = \frac{z_{\mathrm{eq}}+1}{z_c+1}M_i$$

This means not all EDO constraints map to primordial power spectrum constraints

- $f_{\mathrm{DM}} < 1$ for
  - CMB accretion (generalised to larger EDOs)
  - Wide binary evaporation
  - "ICARUS" microlensing (generalised from PBHs to EDOs)

Ramirez and Buckley, MNRAS, arXiv:2209.08100

Bringmann, DC, Sevillano Muñoz, arXiv:2506.XXXX

The primordial power spectrum

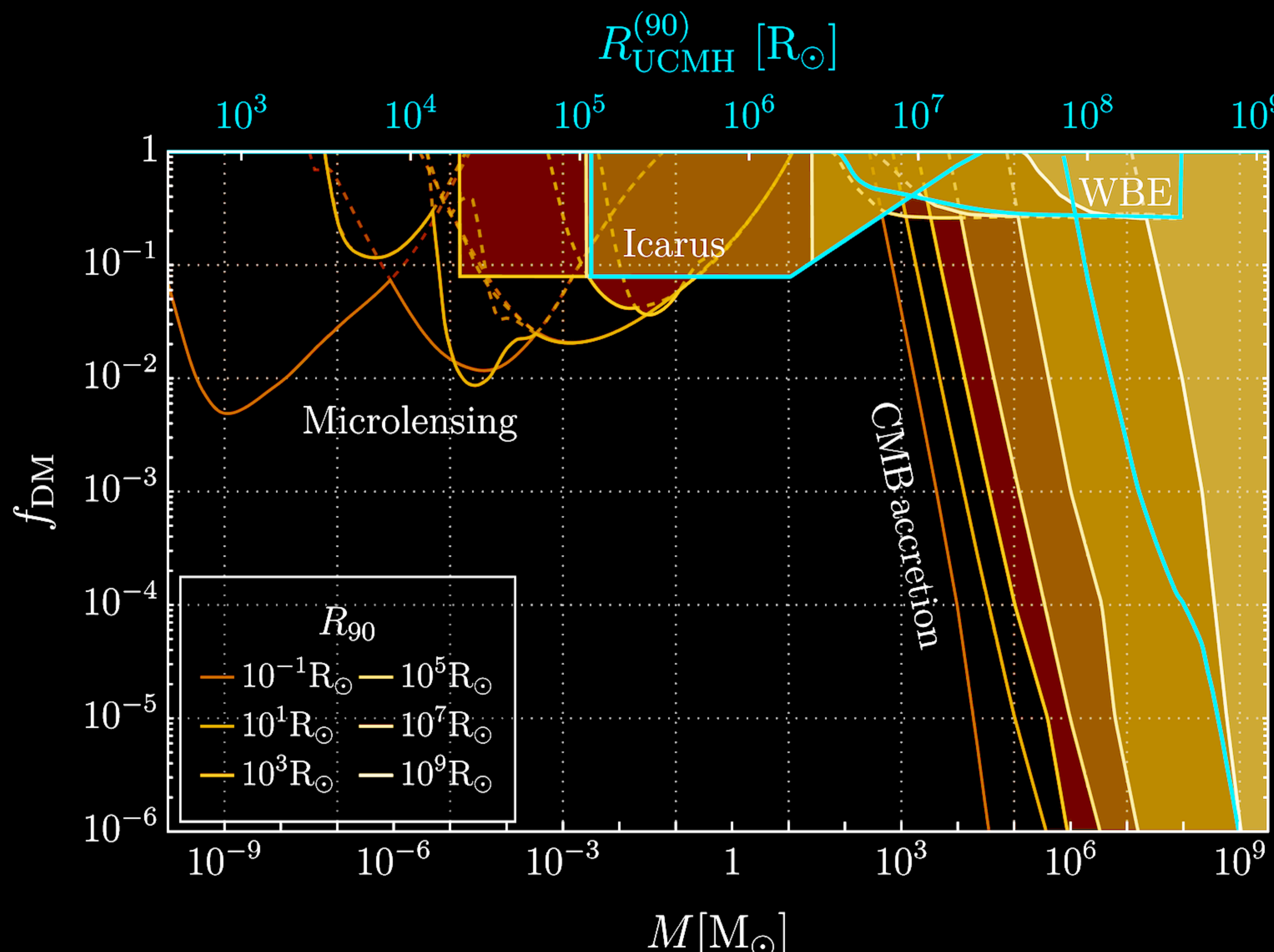

Bringmann, DC, Sevillano Muñoz, arXiv:2506.XXXX

The primordial power spectrum

for UCMH collapsing at z_c, $\frac{R(z_c)}{\mathrm{pc}} = 0.019\left(\frac{1000}{z_c+1}\right)\left(\frac{M(z_c)}{M_\odot}\right)^{1/3}$ with $M(z_c) = \frac{z_{\rm eq}+1}{z_c+1}M_i$

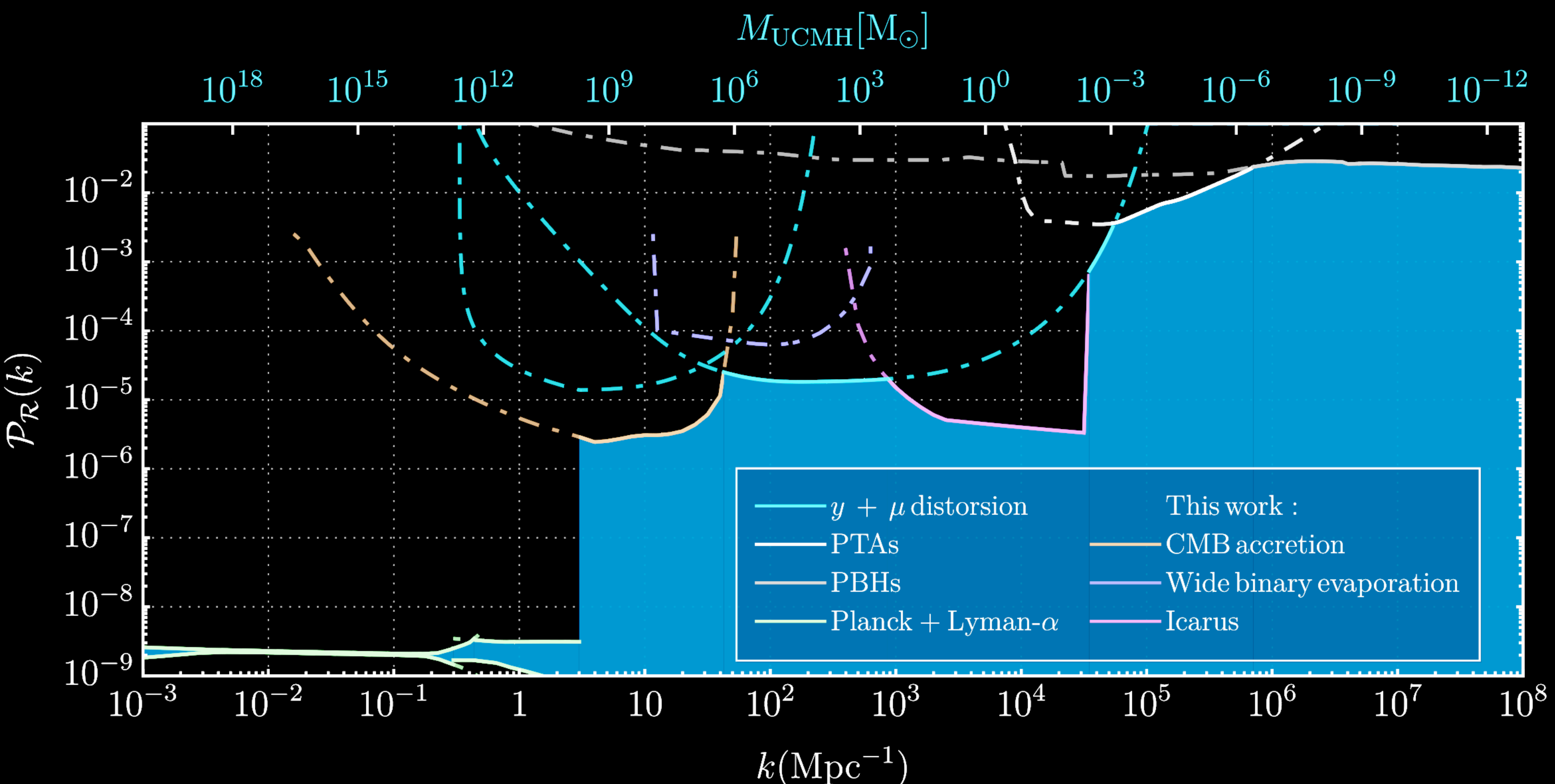

To conclude,

- All of our current evidence for Dark Matter is gravitational; many dark matter models feature substructure
- Microlensing provides a way to look for dark matter substructure of a large range of sizes and masses
  - →Extended objects may give unique microlensing signatures
  - →Non-observation can be used to derive constraints

To conclude,

- All of our current evidence for Dark Matter is gravitational; many dark matter models feature substructure
- Microlensing provides a way to look for dark matter substructure of a large range of sizes and masses
  - →Extended objects may give unique microlensing signatures
  - →Non-observation can be used to derive constraints
- Microlensing signatures of extended objects can be distinguished using machine learning
  - Anomaly detection finds events early in wide-field surveys

To conclude,

- All of our current evidence for Dark Matter is gravitational; many dark matter models feature substructure
- Microlensing provides a way to look for dark matter substructure of a large range of sizes and masses
  - → Extended objects may give unique microlensing signatures
  - → Non-observation can be used to derive constraints
- Microlensing signatures of extended objects can be distinguished using machine learning
  - Anomaly detection finds events early in wide-field surveys
- Gravitational constraints on EDOs lead to constraints on the primordial power spectrum

Many opportunities for future work!

Thank you!

…ask me anything you like!

djuna.l.croon@durham.ac.uk | djunacroon.com

Back up slides

Extended sources: $r_E = \theta_E D_L \sim r_S$

Same procedure as before, but now $u_{1.34}$ is a function of both r_{90} and r_S

DC, D. McKeen, N. Raj, Z. Wang, PRD, arXiv:2007.12697 [astro-ph.CO]

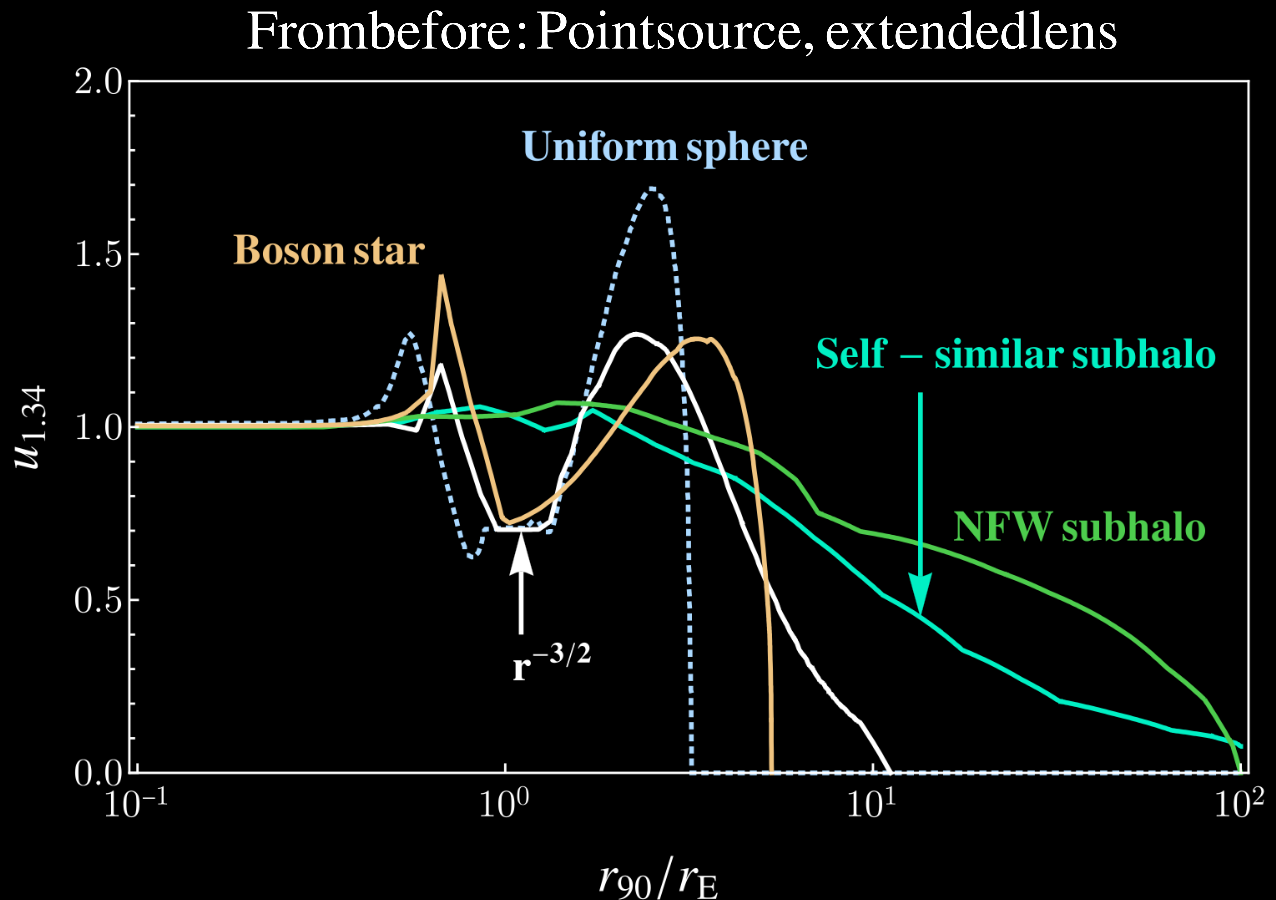

+

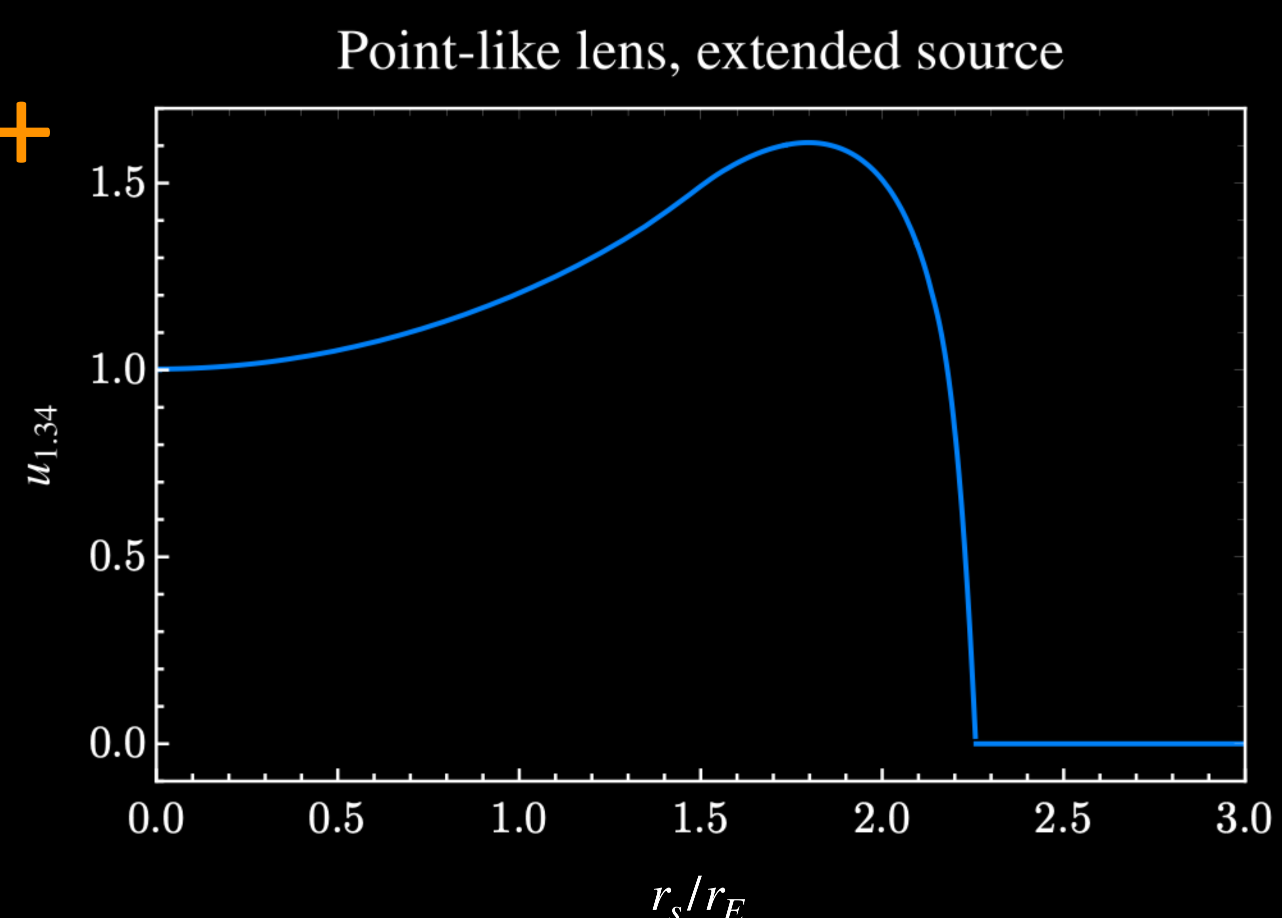

For point-like lenses, see for example,
Witt and Mao, Astrophys. J (1994);
Montero-Camacho, Fang, Vasquez, Silva, Hirata, [JCAP, arXiv:1906.05950];
Smyth, Profumo, English, Jeltema, McKinnon, Guhathakurta [PRD, arXiv:1910.01285];

Extended sources: $r_E = \theta_E D_L \sim r_S$

Same procedure as before, but now $u_{1.34}$ is a function of both r_{90} and r_S

DC, D. McKeen, N. Raj, Z. Wang, PRD, arXiv:2007.12697 [astro-ph.CO]

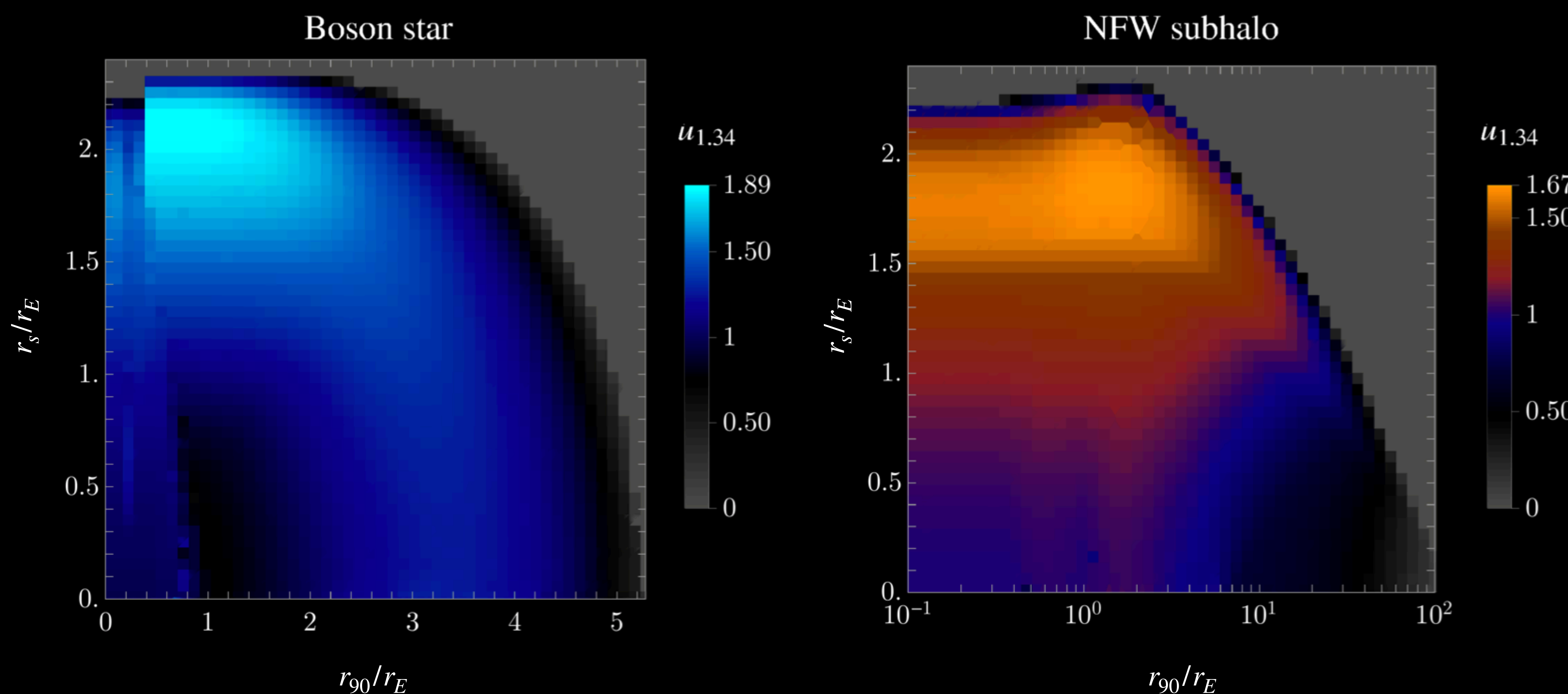

Case study 1: NFW-halo mass profile

- Well-known halo profile: $\rho(r) = \dfrac{\rho_s}{(r/r_s)(1 + r/r_s)^2}$
- As the mass inclosed formally diverges, we cut it off at $R_{cut} = 100R_{sc}$
- Enclosed mass $\propto \log(\kappa + 1) - (\kappa/(\kappa + 1))$ where $\kappa = R_{cut}/R_{sc}$
- Computing $m(\tau)$ is then a trivial exercise:

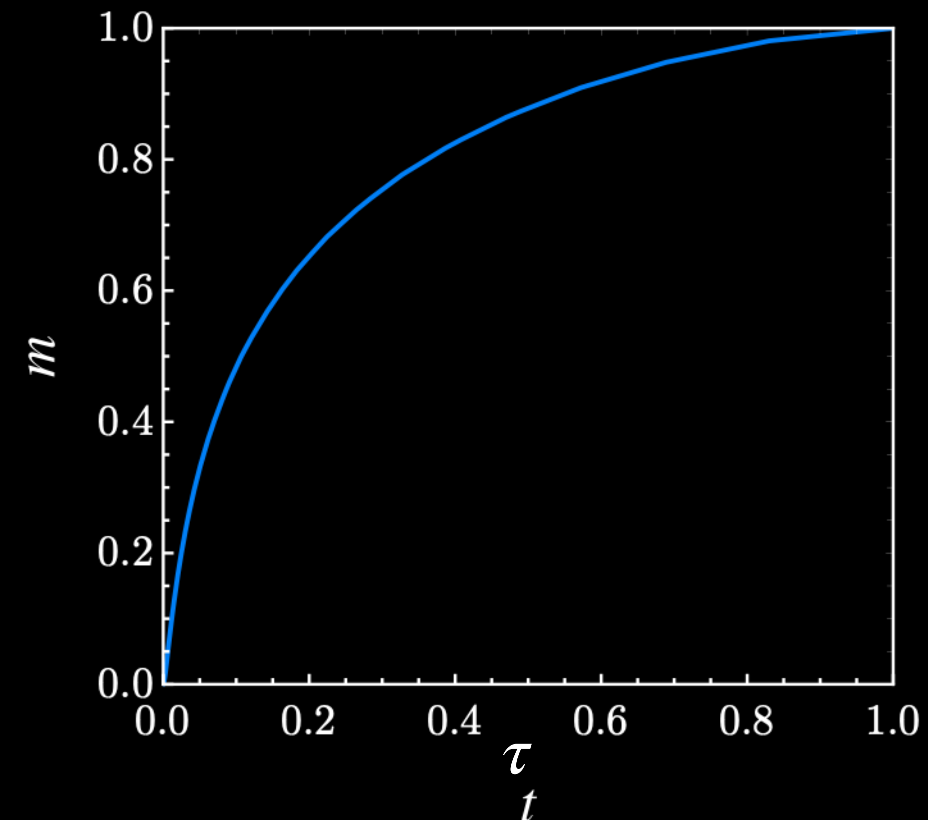

Case study 2: Boson star mass profile

- The Schrodinger-Poisson equation,

$$\mu\Psi = -\frac{1}{2m_\phi}\left(\Psi'' + \frac{2}{r}\Psi'\right) + m_\phi \Phi \Psi$$

Describes the radial distribution

describes a *spherically symmetric ground state of a free scalar field in the non-relativistic limit*

- The mass enclosed is given by

$$M_{\text{BS}}(r) = \frac{1}{m_\phi G}\int_0^{m_\phi r} dy y^2 \Psi^2(y)$$

from which $m(\tau)$ may be computed

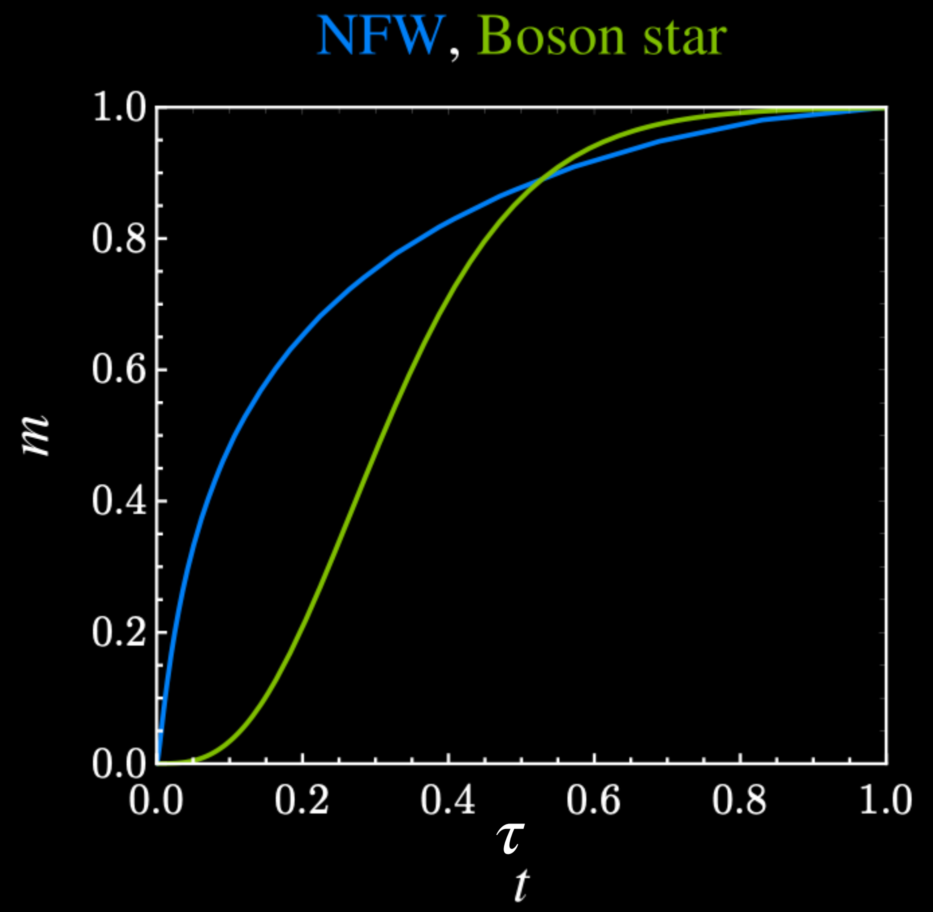

Caustics

Consequence: the Einstein tube is not a tube; not ellipsoidal

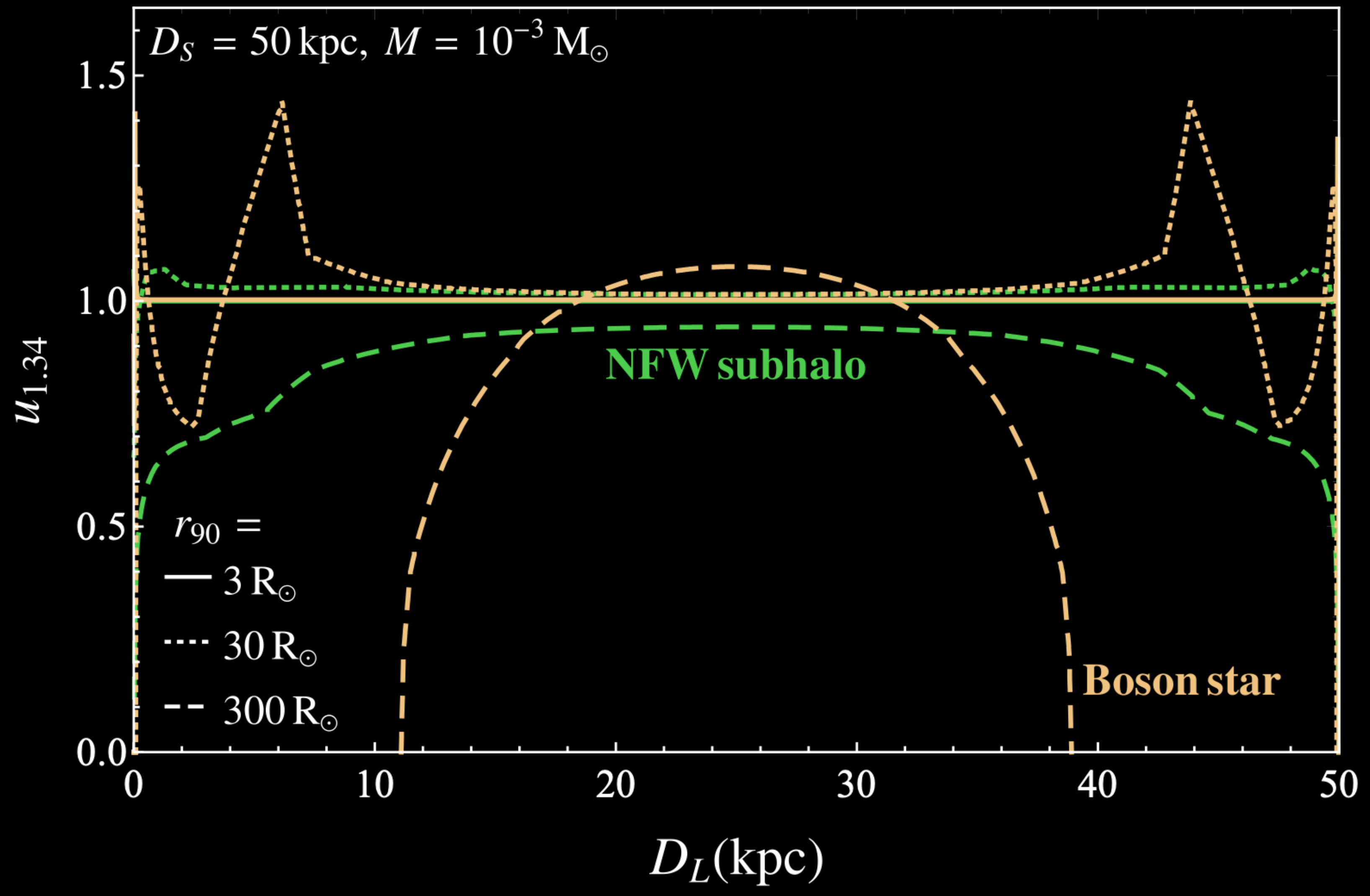

→ Depending on the source, experiments may be more or less sensitive to extended objects compared to point sources in different locations

Obtaining constraints

To obtain limits, we have to account for the observed events

- EROS-2: 3.9 events at 90% CL
- OGLE-IV: $\mathcal{O}(1000)$ astrophysical events, Poissonian 90% CL: $\kappa = 4.61$

$$N_i^{\mathrm{SIG}} \equiv N_i^{\mathrm{FG}} + N_i^{\mathrm{DM}}$$

Bin events in $\mathrm{t_E}$

$$\kappa = 2 \sum_{i=1}^{N_{\mathrm{bins}}} \left[N_i^{\mathrm{FG}} - N_i^{\mathrm{SIG}} + N_i^{\mathrm{SIG}} \ln \frac{N_i^{\mathrm{SIG}}}{N_i^{\mathrm{FG}}} \right]$$

Lensing geometry

- Up to this point, we have assumed that the sources are point-like light sources (a good approximation for EROS/OGLE)
- This approximation breaks down when $r_E = \theta_E D_L \sim r_S$

- Geometry in the lens plane:

$r_s \equiv x R_\star / r_E$

$\bar{u}(\varphi) = \sqrt{u^2 + r_S^2 + 2 u r_S \cos\varphi}$

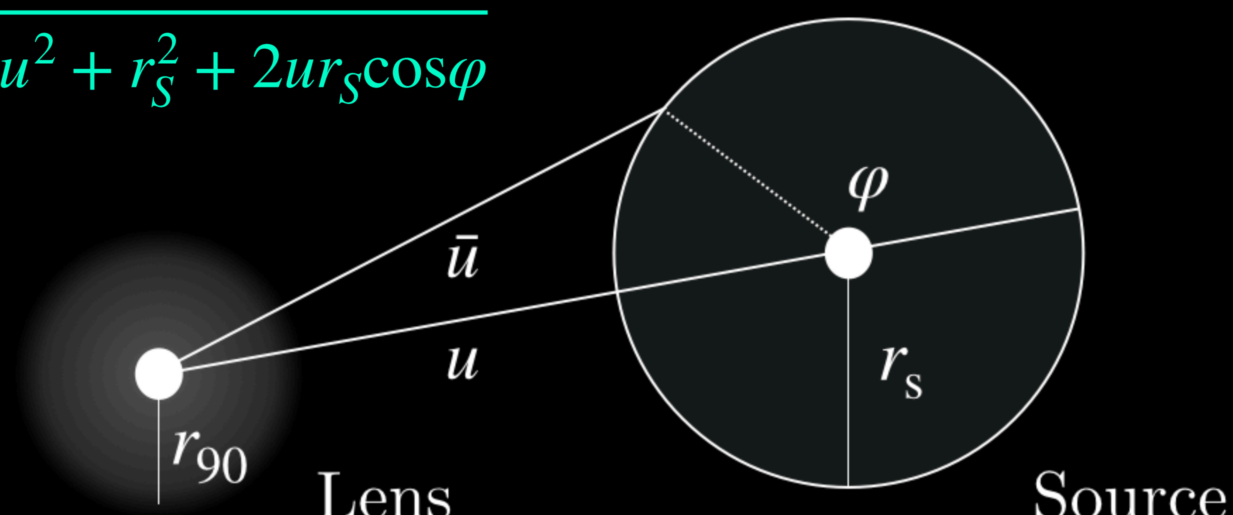

Lensing equation:

$$\bar{u}(\varphi) = \tau(\varphi) - \frac{m(\tau(\varphi))}{\tau(\varphi)}$$

Image parity

Image position

$$\mu_i = \eta \frac{1}{\pi r_S^2} \int_0^{2\pi} d\varphi \frac{1}{2} \tau_i^2(\varphi)$$

Star sizes in M31

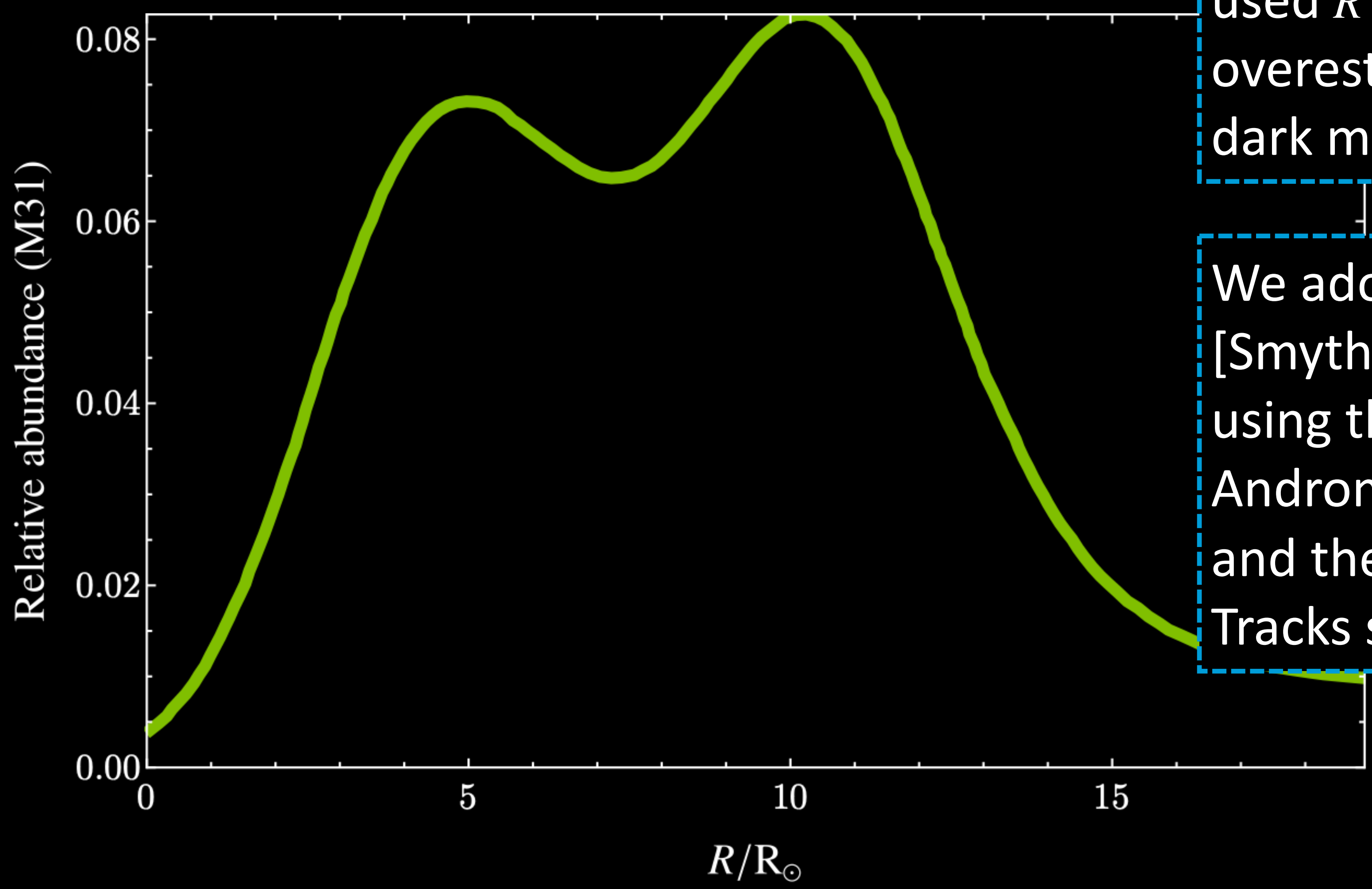

Initially, the Subaru-HSC collaboration used $R = \mathrm{R}_\odot$ for all stars, but this overestimates the constraints on the dark matter fraction

We adopt the distribution derived in [Smyth et al., PRD, arXiv:1910.01285] using the Panchromatic Hubble Andromeda Treasury star catalogue and the `MESA` Isochrones and Stellar Tracks stellar evolution package

$$N_{\mathrm{events}} = N_\star T_{\mathrm{obs}} \int dt_{\mathrm{E}} \int dR_\star \int_0^1 dx \frac{d^2\Gamma}{dx\, dt_{\mathrm{E}}} \frac{dn}{dR_\star}$$

Opportunities for positive detection

M. Crispim-Romao, DC, PRD, arXiv:2402.00107

Caustics arise for $0.8 < \tau_m < 3$

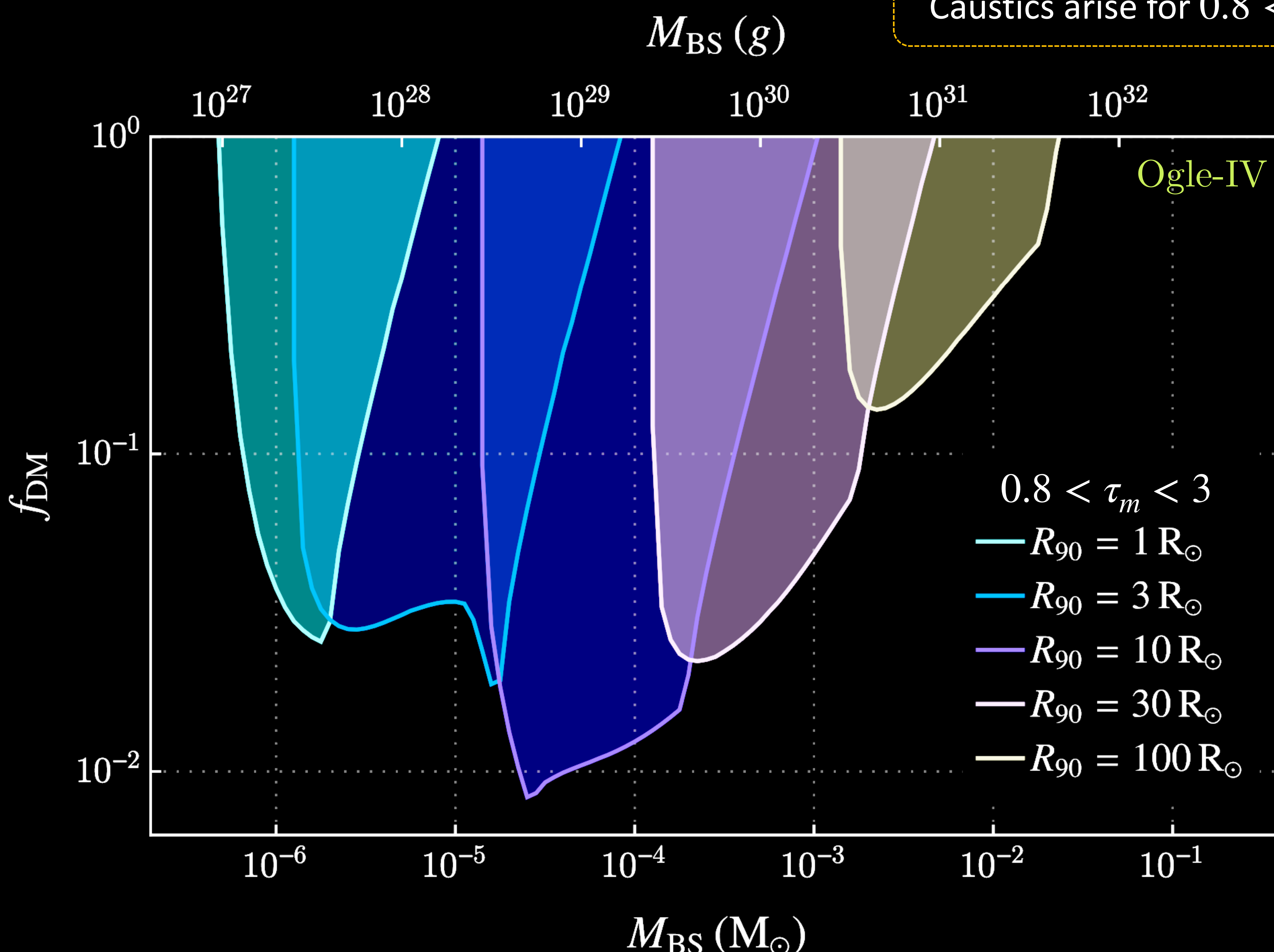

Feature importance

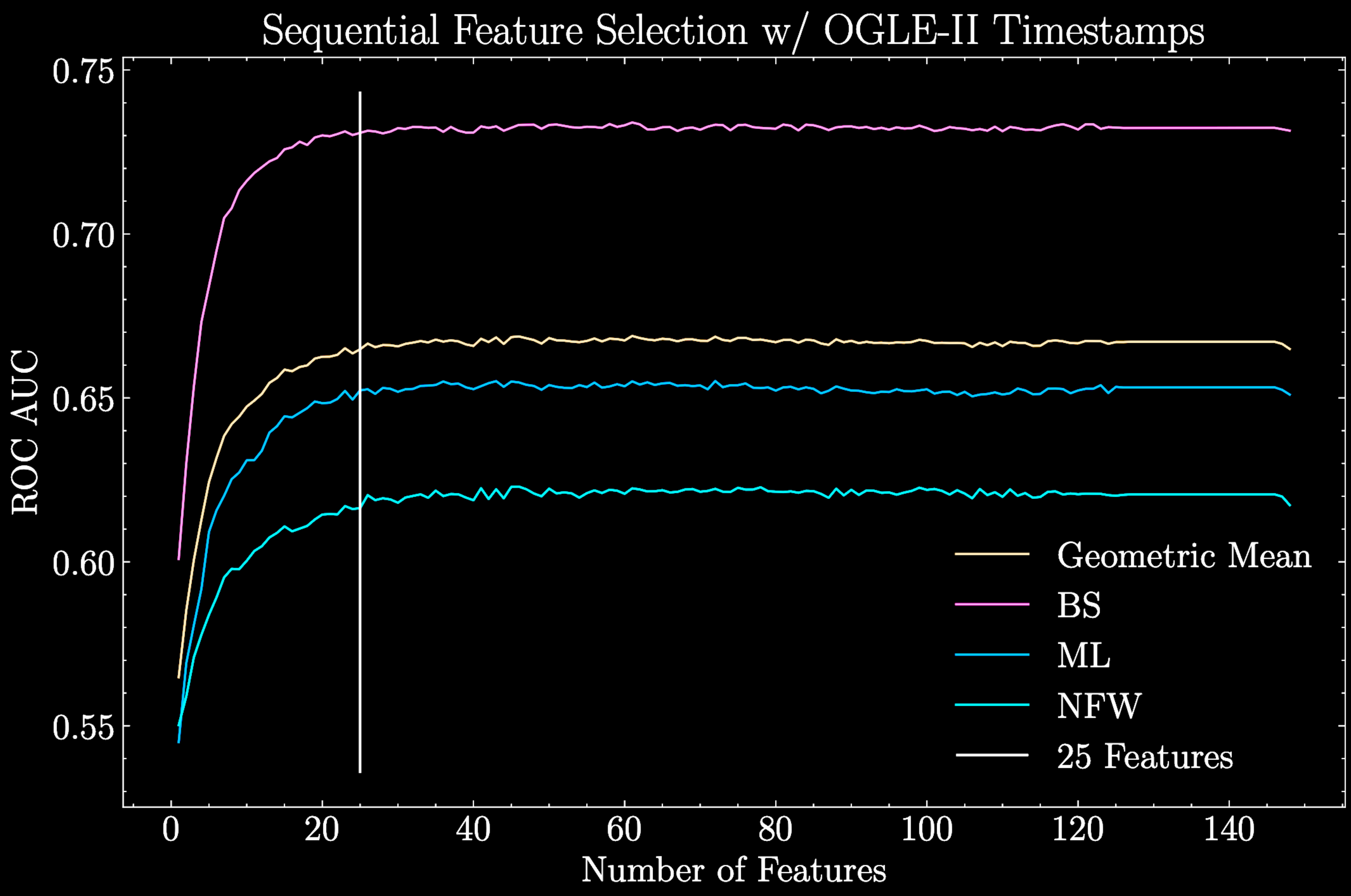

Let's dream…

- The OGLE time steps are quite irregular
- Many different factors play a role…
  - Observational Constraints (weather, moon phase, …)
  - Resource Allocation
  - Target Prioritization
  - Technical Maintenance and Downtime

- But it is interesting what the effect of cadence (ir)regularity is on the observational prospects
- So, let us imagine for a moment that we could achieve perfect daily cadence

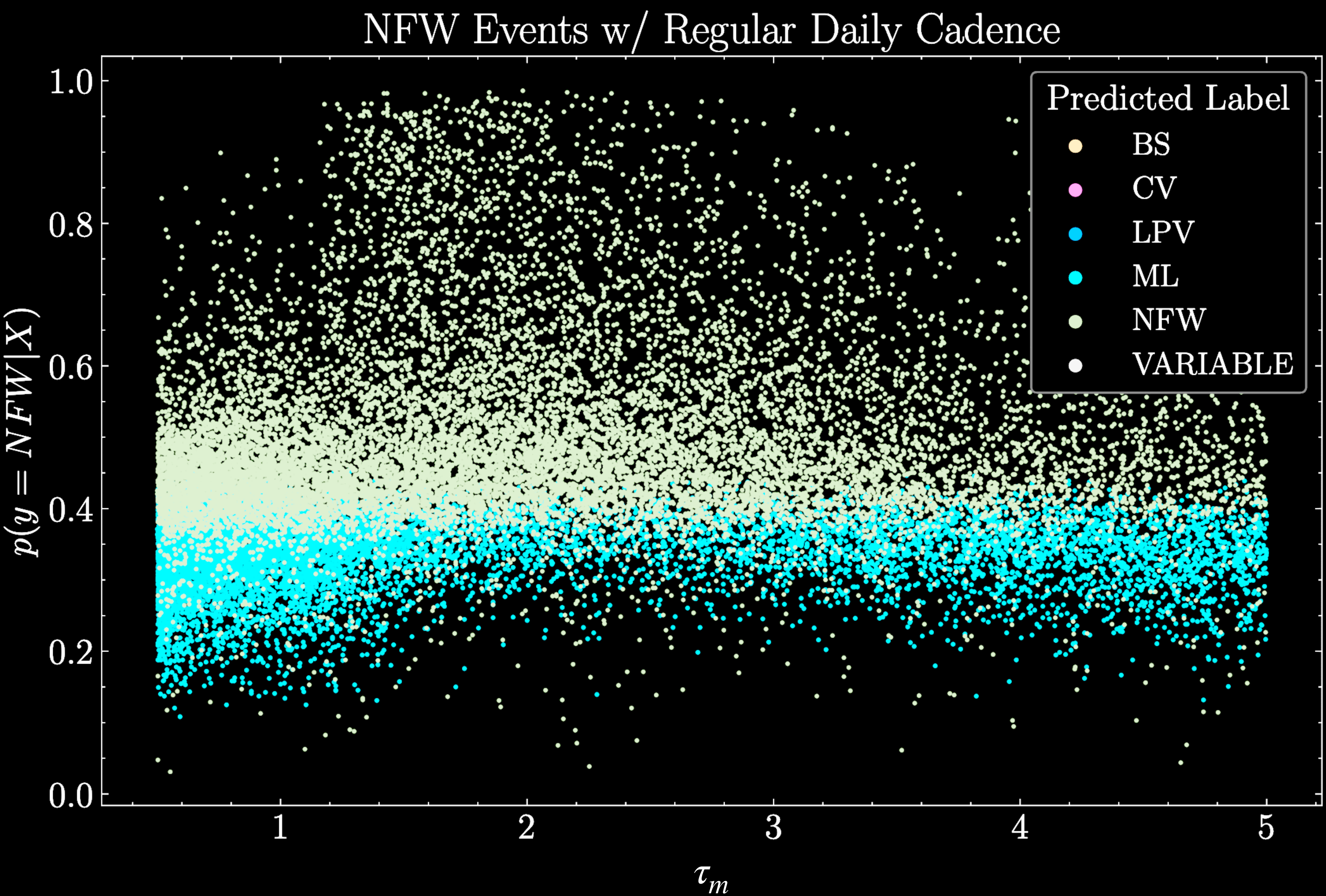

Miguel Crispim-Romao, DC, arXiv:2402.00107

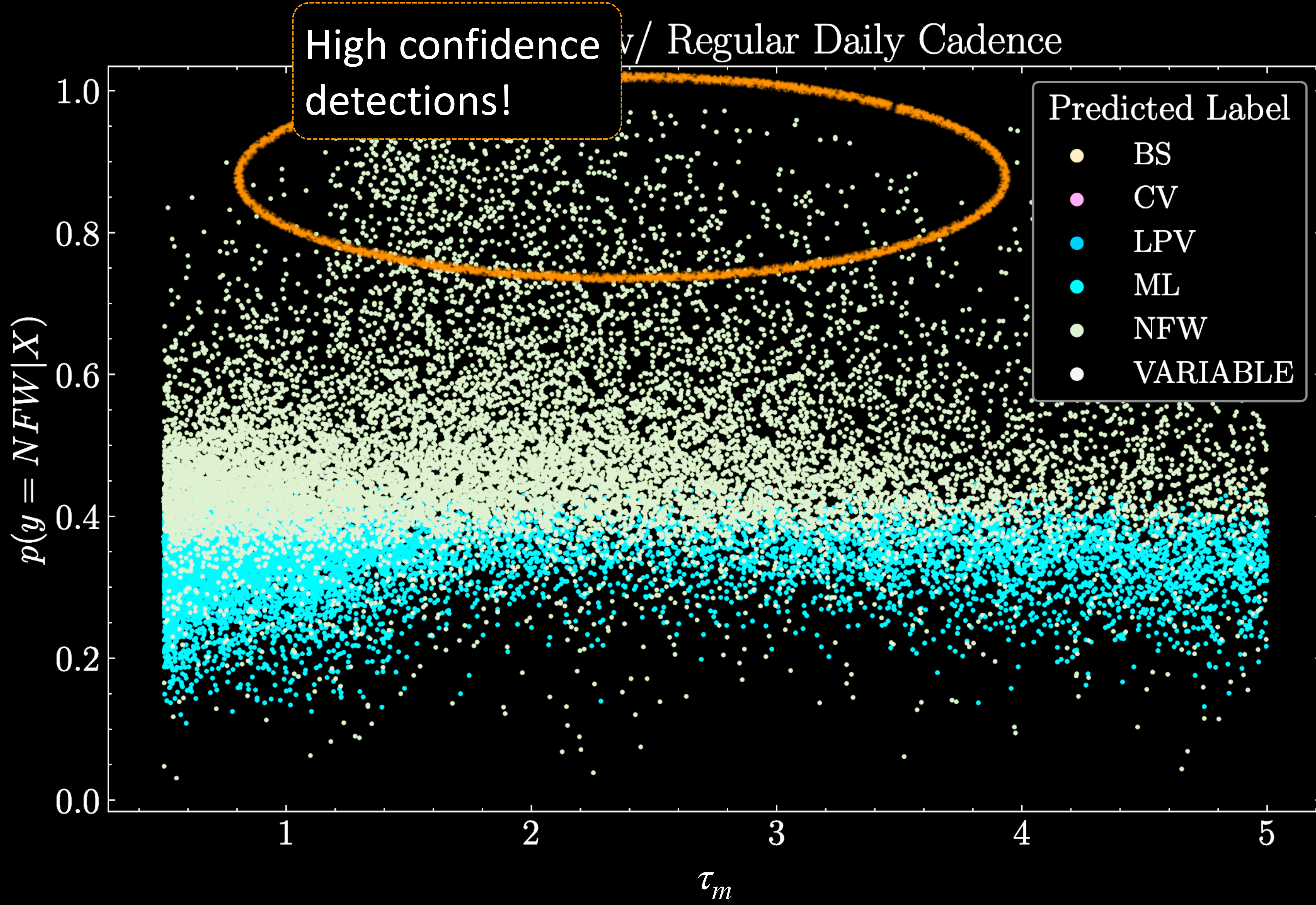

… only observed if regular cadence is achieved

Miguel Crispim-Romao, DC, arXiv:2402.00107